



MACS® Solutions for dermatology research

Find out more about immune cells in dermatology

► miltenyibiotec.com/dermatology



The 3BP2 Adapter Protein Is Required for Chemoattractant-Mediated Neutrophil Activation

This information is current as of July 31, 2012.

Grace Chen, Ioannis Dimitriou, Laura Milne, Karl S. Lang, Philipp A. Lang, Noah Fine, Pamela S. Ohashi, Paul Kubers and Robert Rottapel

J Immunol published online 18 July 2012

<http://www.jimmunol.org/content/early/2012/07/18/jimmunol.1103184>

Supplementary Material <http://www.jimmunol.org/content/suppl/2012/07/18/jimmunol.1103184.DC1.html>

Subscriptions Information about subscribing to *The Journal of Immunology* is online at: <http://jimmunol.org/subscriptions>

Permissions Submit copyright permission requests at: <http://www.aai.org/ji/copyright.html>

Email Alerts Receive free email-alerts when new articles cite this article. Sign up at: <http://jimmunol.org/cgi/alerts/etoc>

The Journal of Immunology is published twice each month by The American Association of Immunologists, Inc., 9650 Rockville Pike, Bethesda, MD 20814-3994. Copyright © 2012 by The American Association of Immunologists, Inc. All rights reserved. Print ISSN: 0022-1767 Online ISSN: 1550-6606.



The 3BP2 Adapter Protein Is Required for Chemoattractant-Mediated Neutrophil Activation

Grace Chen,^{*,†,1} Ioannis Dimitriou,^{*,†,1} Laura Milne,[‡] Karl S. Lang,^{§,¶} Philipp A. Lang,^{†,§} Noah Fine,^{†,||} Pamela S. Ohashi,^{*,†,||} Paul Kubes,[‡] and Robert Rottapel^{*,†,||,#,***}

3BP2 is a pleckstrin homology and Src homology 2 domain-containing adapter protein mutated in cherubism, a rare autosomal-dominant human bone disorder. Previously, we have demonstrated a functional role for 3BP2 in peripheral B cell development and in peritoneal B1 and splenic marginal zone B cell-mediated Ab responses. In this study, we show that 3BP2 is required for G protein-coupled receptor-mediated neutrophil functions. Neutrophils derived from 3BP2-deficient (*Sh3bp2*^{-/-}) mice failed to polarize their actin cytoskeleton or migrate in response to a gradient of chemotactic peptide, fMLF. *Sh3bp2*^{-/-} neutrophils failed to adhere, crawl, and emigrate out of the vasculature in response to fMLF superfusion. 3BP2 is required for optimal activation of Src family kinases, small GTPase Rac2, neutrophil superoxide anion production, and for *Listeria monocytogenes* bacterial clearance in vivo. The functional defects observed in *Sh3bp2*^{-/-} neutrophils may partially be explained by the failure to fully activate Vav1 guanine nucleotide exchange factor and properly localize P-Rex1 guanine nucleotide exchange factor at the leading edge of migrating cells. Our results reveal an obligate requirement for the adapter protein 3BP2 in G protein-coupled receptor-mediated neutrophil function. *The Journal of Immunology*, 2012, 189: 000–000.

Neutrophils are highly motile cells that play an essential role in the innate immune response by phagocytosing, killing, and digesting microbial pathogens. Neutrophils are the most abundant leukocyte found in blood, with $\sim 5 \times 10^6$ cells per milliliter of blood in humans (1), and they are usually the first cells recruited to the sites of infection (1). Neutropenia or syndromes that compromise neutrophil function are associated with increased susceptibility to bacterial or fungal infections (2).

Mobilization of neutrophils to sites of infection is orchestrated by the elaboration of bacterial-derived peptides such as *N*-formylmethionyl oligopeptides fMLF (3), the production of IL-8 by phagocytes (4), and the activation of the complement system with the local release of fragment C5a (5). These factors are ligands for heptahelical, heterotrimeric G protein-coupled receptors (GPCRs) on the surface of neutrophils, which trigger the production of reactive oxygen species (ROS), the exocytosis of antimicrobial

factors, and migratory behavior of neutrophils into sites of inflammation. G proteins are composed of α , β , and γ subunits. Based on their sequence and functional similarities, the α subunits can be grouped into four families: $G\alpha_s$, $G\alpha_i$, $G\alpha_q$, and $G\alpha_{12}$ (6). Ligand-bound receptors activate G proteins by catalyzing the exchange of GDP bound to the α subunit with GTP, resulting in dissociation of the GTP-bound $G\alpha$ subunit from the $G\beta\gamma$ subunit complex (7). The GTP- $G\alpha$ and the free $G\beta\gamma$ subunit interact with their respective effector proteins that further amplify the signal. GPCR activation triggers rapid protein tyrosine phosphorylation in neutrophils (8, 9), and treatment with inhibitors of tyrosine kinases blocks neutrophil responses to chemoattractants (10, 11). Among cytosolic tyrosine kinases, members of the Src family have been implicated in fMLF-mediated signal transduction (12–14). Neutrophils derived from *Hck/Fgr*-deficient mice or human neutrophils treated with the Src kinase inhibitor 4-amino-5-(4-chlorophenyl)-7-(*t*-butyl)pyrazolo[3,4-*d*]pyrimidine (15) demonstrated a critical role for Src kinase in fMLF-mediated respiratory burst and formation of F-actin (16). GPCR ligation also leads to activation of lipid kinases, guanine nucleotide exchange factors (GEFs), and small GTPases (17). The Ras-related small GTPase family, including Rac1, Rac2, RhoA, and Cdc42, is key in regulating many chemoattractant-mediated neutrophil responses (18–26). Among the Rho GTPase subfamily, Rac2 is uniquely required for both fMLF-mediated chemotaxis and superoxide production of neutrophils (19, 20, 27, 28). Studies using mutant mice have identified several Rac2 GEFs, including DOCK2 (29), GIT2 (30), and P-Rex1 (31), required for neutrophil function. Whereas DOCK2 and GIT2 regulate both Rac1 and Rac2 activities (29, 30), genetic data suggest that P-Rex1 functions as a predominant Rac2 GEF in mouse neutrophils (31). P-Rex1-deficient neutrophils demonstrate a selective defect in Rac2 activation following fMLF stimulation, and P-Rex1^{-/-} neutrophils phenocopy many of the functional defects observed in Rac2^{-/-} cells (19, 27, 31).

The role of adapter proteins in GPCR signaling has not been extensively examined. We and others have identified 3BP2 as a binding protein of c-Abl (32), Syk (33), and Vav (34). 3BP2 is

*Department of Immunology, University of Toronto, Toronto, Ontario M5S 148, Canada; [†]Campbell Family Institute for Breast Cancer Research, Ontario Cancer Institute, University Health Network, Toronto, Ontario M5G 2C1, Canada; [‡]Immunology Research Group, Department of Physiology and Biophysics, Institute of Infection, Immunity and Inflammation, University of Calgary, Calgary, Alberta T2N 4N1, Canada; [§]Department of Gastroenterology, Hepatology and Infectious Diseases, Heinrich Heine University, 40225 Duesseldorf, Germany; [¶]Institute for Immunology, University of Essen, 45147 Essen, Germany; ^{||}Department of Medical Biophysics, University of Toronto, Toronto, Ontario M5G 2M9, Canada; [#]Department of Medicine, University of Toronto, Toronto, Ontario M5G 2C4, Canada; and ^{***}St. Michael's Hospital, Toronto, Ontario M5B 1W8, Canada

¹G.C. and I.D. contributed equally to the manuscript.

Received for publication November 15, 2011. Accepted for publication June 19, 2012.

Address correspondence and reprint requests to Dr. Robert Rottapel, Ontario Cancer Institute, Princess Margaret Hospital, 610 University Avenue, Room 10-108, Toronto, Ontario M5G 2M9, Canada. E-mail: rottapel@oci.utoronto.ca

The online version of this article contains supplemental material.

Abbreviations used in this article: BM, bone marrow; GEF, guanine nucleotide exchange factor; GPCR, G protein-coupled receptor; PBD, p21 binding domain; PIP₃, phosphatidylinositol 3,4,5-triphosphate; ROS, reactive oxygen species.

Copyright © 2012 by The American Association of Immunologists, Inc. 0022-1767/12/\$16.00

composed of an N-terminal pleckstrin homology domain followed by a proline-rich region, and a C-terminal Src homology 2 domain. We have previously reported that 3BP2 is required for optimal B cell activation (35) and osteoclast and osteoblast function (36). In this study, we report that in the absence of 3BP2, neutrophils fail to polarize their actin cytoskeleton and migrate toward an fMLF gradient in vitro and fail to crawl to optimal sites of emigration in response to fMLF superfusion in vivo. Neutrophils lacking 3BP2 are unable to release optimal levels of superoxide anion in response to fMLF in vitro, and 3BP2-deficient mice are defective in efficiently clearing *Listeria monocytogenes* bacterial infection. In addition to defects in F-actin polarization, we also demonstrate a failure of *Sh3bp2*^{-/-} neutrophils to accumulate P-Rex1 at the leading edge during chemotaxis in response to an fMLF gradient. We show that 3BP2 is required for full activation of Src family kinases, Vav1, Rac2, Pak, and Erk kinases following fMLF stimulation. 3BP2 is therefore an adapter protein that links fMLF-induced receptor-proximal signaling events to the actin cytoskeleton and NADPH oxidase complex in neutrophils required for effective bactericidal function in vivo.

Materials and Methods

Sh3bp2 gene-targeted mice

Sh3bp2^{+/+} and *Sh3bp2*^{-/-} mice were generated as described previously (35). Mice used in all experiments were in F₇ backcross generation and were maintained at the animal facilities of the Ontario Cancer Institute under specific pathogen-free conditions according to University Health Network Animal Care Committee Guidelines.

Abs

Western blotting was performed using the following primary Abs: anti-phospho-Src family (Tyr⁴¹⁶), anti-Src, anti-phospho-PAK1 (Thr⁴²³)/PAK2 (Thr⁴⁰²), anti-phospho-PAK1 (Ser¹⁹⁹)/PAK2 (Ser¹⁹²), anti-PAK1, anti-PAK2, anti-phospho-p44/42 (Erk1/Erk2) (Thr²⁰²/Tyr²⁰⁴), anti-Erk1/Erk2, anti-phospho-p38 (Thr¹⁸⁰/Tyr¹⁸²), anti-p38, anti-phospho-Akt (Ser⁴⁷³), and anti-Akt were all purchased from Cell Signaling Technology. Anti-Vav1 (C-14) and anti-phosphotyrosine Abs (pY99) were purchased from Santa Cruz Biotechnology. Abs used to immunoprecipitate 3BP2 and detect 3BP2 on Western blots were generated as described (35). HRP-conjugated anti-mouse or anti-rabbit secondary Abs were from Amersham Pharmacia Biotech.

Isolation of bone marrow neutrophils

Mouse bone marrow (BM) neutrophils were isolated from femurs and tibiae as described by Lowell et al. (37). Briefly, marrow cells were flushed from bones using HBSS (without Ca⁺⁺/Mg⁺⁺) plus 0.1% BSA followed by lysing RBCs with 0.155 M NH₄Cl, 10 mM KHCO₃, and 0.1 mM EDTA. The remaining leukocytes were washed twice with Ca⁺⁺/Mg⁺⁺-free HBSS and resuspended in 3 ml 45% Percoll (Amersham Biosciences) solution in Ca⁺⁺/Mg⁺⁺-free HBSS. A portion of the cell suspension was used for Gr-1 staining using PE-labeled anti-Gr-1 Ab to determine the percentage of Gr-1⁺ cells in BM of *Sh3bp2*^{+/+} and *Sh3bp2*^{-/-} mice. The rest of the cell suspension was loaded on top of a Percoll density gradient prepared in a 15-ml polystyrene tube by layering successively 2 ml 62, 55, and 50% Percoll solutions on top of 3 ml 81% Percoll solution. Cells were then centrifuged at 2500 rpm for 30 min at room temperature. The cell band formed between the 81 and 62% layer was harvested using a Pasteur pipette and washed twice with Ca⁺⁺/Mg⁺⁺-free HBSS plus 0.1% BSA. The isolated mature neutrophils were resuspended in Ca⁺⁺/Mg⁺⁺-containing HBSS before each of the experiments unless otherwise indicated. FACS analysis of cell preparations revealed high expression of murine granulocyte marker Gr-1 on ~80–90% of the cells isolated from the 62–81% interface.

Blood neutrophil cell count

Blood was collected from the tails of 9- to 11 wk-old mice using EDTA-coated capillary tubes and transferred to Eppendorf tubes. Blood was allowed to mix with EDTA in Eppendorf tubes for 30 min at room temperature. The samples were analyzed using a Hemavet 950 (Drew Scientific Group) by the Toronto Center for Phenogenomics.

Chemotaxis assay

BM neutrophils were resuspended in HBSS plus 1% gelatin at 5 × 10⁶ cells/ml. The cell suspension was allowed to attach to BSA-coated glass coverslips (22 × 40 mm) at 37°C for 20 min. The coverslip was inverted onto a Zigmund chamber (Neuro Probe), and 100 μl HBSS media was added to the left chamber with 100 μl HBSS media containing 10 μM fMLF (Sigma-Aldrich) added to the right chamber. Neutrophil movement in Zigmund chambers was recorded with time-lapse video microscopy (Nikon upright Optiphot). Images were captured at 60-s intervals with a Nikon CoolSNAP-Pro color camera. Cell-tracking software (Retrac version 2.1.01 freeware) was used to characterize neutrophil chemotaxis from the captured images.

Actin polymerization and F-actin localization

BM neutrophils were resuspended in HBSS and stimulated with 10 μM fMLF for different time intervals. Cells were immediately fixed with 4% paraformaldehyde, permeabilized with 0.1% Triton X-100, and stained with Alexa Fluor 488-conjugated phalloidin (1 U/500 μl cell suspension; Molecular Probes) to detect F-actin content. Samples were analyzed with a FACSCalibur flow cytometer.

For visualization of F-actin localization, chemotaxing neutrophils (under the 10 μM fMLF gradient) on coverslips were fixed with 4% paraformaldehyde and permeabilized with 0.2% Triton X-100 in PBS. Cells were then incubated in PBS containing 3% BSA and stained with Oregon Green 514-conjugated phalloidin (Molecular Probes). All images were taken with a laser scanning confocal microscope (Zeiss LSM510).

P-Rex1 localization

To visualize P-Rex1 localization, chemotaxing neutrophils (under the 10 μM fMLF gradient) on coverslips were fixed with 4% paraformaldehyde and permeabilized with 0.5% Triton X-100 in PBS. Cells were then incubated in PBS containing 10% donkey serum and stained with 5 μg/ml rat anti-P-Rex1 mAb (a gift from M. Hoshino, Kyoto University, Kyoto, Japan) followed by incubation with secondary, Alexa Fluor 488-conjugated anti-rat IgG (Molecular Probes). The distribution of P-Rex1 was examined with a laser scanning confocal microscope (Zeiss LSM510).

Intravital microscopy

Sh3bp2^{+/+} and *Sh3bp2*^{-/-} male mice were anesthetized with a mixture of 200 mg/kg ketamine hydrochloride (Rogar/STB, Montreal, QC, Canada) and 10 mg/kg xylazine (Bayer HealthCare, Animal Health, Toronto, ON, Canada) injected i.p. The right jugular vein was cannulated for administration of additional anesthetic. The cremaster muscle was used to study the behavior of leukocyte recruitment as previously described (38). Briefly, an incision was made in the scrotal skin to expose the left cremaster muscle, which was exteriorized following dissection from associated tissues and placed on a clear viewing pedestal. A cautery pen was used to make a longitudinal cut in the cremaster muscle, which was then held flat against the pedestal by securing silk sutures to the perimeter of the muscle. The muscle was superfused initially with bicarbonate-buffered saline (pH 7.0, 37°C), followed by superfusion with fMLF (pH 7.0, 37°C). C57BL/6J mice (The Jackson Laboratory) were used as a control for the assay.

The preparation was visualized using an intravital microscope (Axioskop; Carl Zeiss) with a ×25 objective lens (L25/0.35; E. Leitz, Munich, Germany), which was connected to a video camera (5100 HS; Panasonic, Osaka, Japan). The same five sections of single unbranched cremasteric venules (20–40 μm in diameter) were observed throughout the experiment. The images were recorded on a videocassette for video playback analysis to determine rolling flux, rolling velocity, adhesion, and emigration of leukocytes. Rolling leukocytes were defined as those cells moving at a velocity less than that of erythrocytes within a chosen vessel. The rolling flux was measured as the number of leukocytes that pass through a 100-μm section of vessel per minute. The rolling velocity was calculated from the time required for a cell to roll along a 100-μm length of vessel and is expressed as micrometers per second. A cell was deemed adherent when it remained stationary for at least 30 s. Leukocyte emigration constitutes the total number of cells observed in the extravascular space adjacent to the observed venule within the microscopic field of view.

Crawling

Neutrophil crawling within the venules was recorded using a ×40 objective and 72× time-lapse video recorder. Single unbranched venules (20–30 μm in diameter) were imaged before and after fMLF (0.5 μM) superfusion. The crawling distance, crawling velocity, and percentage of adherent cells that crawl were recorded. The time-lapse video (time-lapsed to a total of

900×; 1 frame = 30 s) of crawling cells was tracked manually in an ImagePro 6.2. All crawling was assumed to occur in two dimensions.

Superoxide production

BM neutrophils (1×10^5) resuspended in HBSS were stimulated with 10 μ M fMLF or 1 μ M PMA (Sigma-Aldrich). The chemiluminescence was counted with an enhancer-containing, luminol-based detection system (National Diagnostics) using a luminometer. Superoxide dismutase was added to some samples to be used as negative controls.

L. monocytogenes infection

Nine- to 11-wk-old mice were injected i.v. with 2×10^4 CFU *L. monocytogenes* (clinically isolated wild-type strain 10403s) and sacrificed on day 2 postinfection. Numbers of viable *L. monocytogenes* in livers and spleens of infected animals were determined by plating serial dilution of organ homogenates in PBS on brain–heart-infused agar. For survival assay, mice were injected i.v. with 10^5 CFU *L. monocytogenes*. The end point of the assay is 14 d after infection.

Coimmunoprecipitation, immunoprecipitation, and immunoblotting

BM neutrophils were lysed with ice-cold 1% Triton X-100 lysis buffer (50 mM HEPES [pH 7.0], 150 mM NaCl, 10% glycerol, 1% Triton X-100, 1.5 mM MgCl₂, 1 mM EGTA, 1 mM sodium orthovanadate, 1 mM PMSF, and Roche complete protease inhibitor mixture tablets) for 20 min on ice. Nuclei were pelleted by centrifugation for 10 min at $16,000 \times g$ and 4°C. For immunoprecipitation, lysates were incubated for 2 h with the indicated Abs, followed by incubation with either protein A- or protein G-Sepharose beads (Amersham Biosciences) for 1 h at 4°C. After incubation, pellets were washed five times with ice-cold 0.2% Triton X-100 lysis buffer and resuspended in SDS sample buffer. Eluted immunoprecipitates or whole-cell lysates were resolved by SDS-PAGE, transferred to polyvinylidene difluoride membranes, probed with the indicated primary Abs and HRP-conjugated secondary Abs, and developed using an ECL kit (Amersham Biosciences) according to the manufacturer's instructions. Quantification of band ODs for Western blots was calculated using the Quantity One program (Bio-Rad Laboratories).

PAK-p21 binding domain pull-down assay

BM neutrophils were lysed as described above. Aliquots of the cell extracts were kept for total lysate controls, and the remaining extracts were incubated with GST-fusion, p21 (Cdc42/Rac)-binding domain of PAK1 (GST-PAK1-PBD; Cytoskeleton) at 4°C for 1 h preceded by a 1-h incubation of glutathione agarose beads with GST-PAK1-PBD. The bound proteins and the comparable amount of total lysates were analyzed by SDS-PAGE, and blots were probed with Rac1-specific Ab (BD Transduction Laboratories), Rac2-specific Ab (Upstate Biotechnology), or Cdc42-specific Ab (BD Transduction Laboratories).

Statistical analysis

Averaged numerical data were presented as means \pm SEM. Unless otherwise indicated, a Student *t* test was used to determine the statistical significance of differences between groups. Data for intravital microscopy and crawling experiments are presented as means \pm SEM and analyzed using GraphPad InStat 3 software (GraphPad Software). Unless otherwise noted, results were analyzed using ANOVA with Bonferroni correction. A *p* value of <0.05 was considered statistically significant.

Results

Sh3bp2^{-/-} neutrophils are defective in fMLF-induced chemotaxis

To examine the role of 3BP2 in controlling neutrophil chemotaxis, BM-derived neutrophils from *Sh3bp2*^{+/+} and *Sh3bp2*^{-/-} mice were subjected to time-lapse videomicroscopy to track individual cell migration in response to an fMLF gradient. In the absence of chemoattractants, neither *Sh3bp2*^{+/+} nor *Sh3bp2*^{-/-} neutrophils demonstrated significant cellular movement (data not shown). Addition of fMLF to the cells induced rapid and directionally random movements of both *Sh3bp2*^{+/+} and *Sh3bp2*^{-/-} neutrophils with similar speed (Fig. 1A, left panels). In response to an fMLF gradient, *Sh3bp2*^{+/+} neutrophils moved toward the fMLF gradient,

whereas the *Sh3bp2*^{-/-} neutrophils displayed an indecisive wandering behavior (Rayleigh test of uniformity, *p* value of 3.76×10^{-12} for *Sh3bp2*^{+/+} cells and a *p* value of 0.87 for *Sh3bp2*^{-/-} cells) (Fig. 1A, right panels, 1B). Neutrophils derived from both strains of mice moved at similar speeds of $4.57 \pm 0.36 \mu\text{m}/\text{min}$ (Fig. 1C).

Polymerized F-actin formation provides the primary driving force for neutrophil locomotion, and the accumulation of F-actin at the leading edge of migrating neutrophils correlates with the directional movement of neutrophils (39, 40). We examined both the formation of total F-actin and the location of accumulated F-actin in fMLF-stimulated neutrophils by phalloidin staining using flow cytometry and immunofluorescence. Total cellular F-actin assembled after fMLF stimulation was similar in both *Sh3bp2*^{+/+} and *Sh3bp2*^{-/-} neutrophils (Fig. 1D). However, in response to an fMLF gradient, 40% of wild-type neutrophils reorganized F-actin in a polarized manner at the leading edge of the cell toward the fMLF gradient, whereas only 16% of the *Sh3bp2*^{-/-} neutrophils had polarized F-actin structures by 15 min (Fig. 1E). In no case did the 3BP2-deficient neutrophils demonstrate as compact and highly polarized actin structures as those observed in neutrophils derived from wild-type mice (Fig. 1E). Therefore, 3BP2 is required for directional movement and for the establishment and/or maintenance of asymmetrical polymerized actin in response to fMLF chemotactic gradients.

3BP2 is required for normal neutrophil in vivo chemotaxis to fMLF

To test the capacity of *Sh3bp2*^{-/-} neutrophils to migrate in vivo, we assayed the chemotaxis of *Sh3bp2*^{+/+} and *Sh3bp2*^{-/-} neutrophils within the cremaster muscle in response to superfusion of fMLF. In unstimulated mice, ~50–60 cells/min rolled past a given point on the video screen (Fig. 2A) at a velocity of ~35 $\mu\text{m}/\text{s}$ (Fig. 2B). Both *Sh3bp2*^{+/+} and *Sh3bp2*^{-/-} neutrophils showed comparable basal values for rolling flux (Fig. 2A) and rolling velocity (Fig. 2B). In response to superfusion of fMLF, the rolling flux and rolling velocity decreased similarly for both *Sh3bp2*^{+/+} and *Sh3bp2*^{-/-} groups (Fig. 2A, 2B). However, although neutrophil adhesion in *Sh3bp2*^{+/+} mice increased 6-fold during the course of 60 min in response to fMLF superfusion, neutrophil adhesion in *Sh3bp2*^{-/-} mice increased only 3-fold during the same duration (Fig. 2C). Emigration increased 4-fold in *Sh3bp2*^{+/+} after 60 min of fMLF superfusion whereas *Sh3bp2*^{-/-} neutrophils exhibited 50% less emigration than was seen in *Sh3bp2*^{+/+} neutrophils (Fig. 2D).

Given defective adhesion and emigration of *Sh3bp2*^{-/-} neutrophils in response to fMLF superfusion in vivo, time-lapse microscopy was performed to elucidate the restricted emigration of *Sh3bp2*^{-/-} neutrophils. We observed that virtually 100% of *Sh3bp2*^{+/+} neutrophils that adhered to the vessel wall crawled along the venule lumen and subsequently emigrated out of the vessel. In comparison, the *Sh3bp2*^{-/-} neutrophils that adhered to the vessel luminal wall successfully were defective in their ability to crawl to final emigration sites (Fig. 2E). Only ~40% of *Sh3bp2*^{-/-} neutrophils were capable of crawling following adhesion (Fig. 2E) and crawled at a reduced velocity (30% less than that of *Sh3bp2*^{+/+} cells) covering a shorter distance compared with *Sh3bp2*^{+/+} cells (half of the distance traveled by *Sh3bp2*^{+/+} cells) (Fig. 2F, 2G). These results demonstrated that 3BP2 is required for optimal neutrophil adhesion to the vessel wall, as well as crawling and emigration toward fMLF in vivo.

We next investigated whether the transendothelial migratory defect in 3BP2-deficient neutrophils was due in part to a cell nonautonomous function of 3BP2 in endothelial cells given that 3BP2 is expressed in endothelial cells (Supplemental Fig. 1A). To test the integrity of the endothelial barrier in the absence of 3BP2, we adoptively transferred

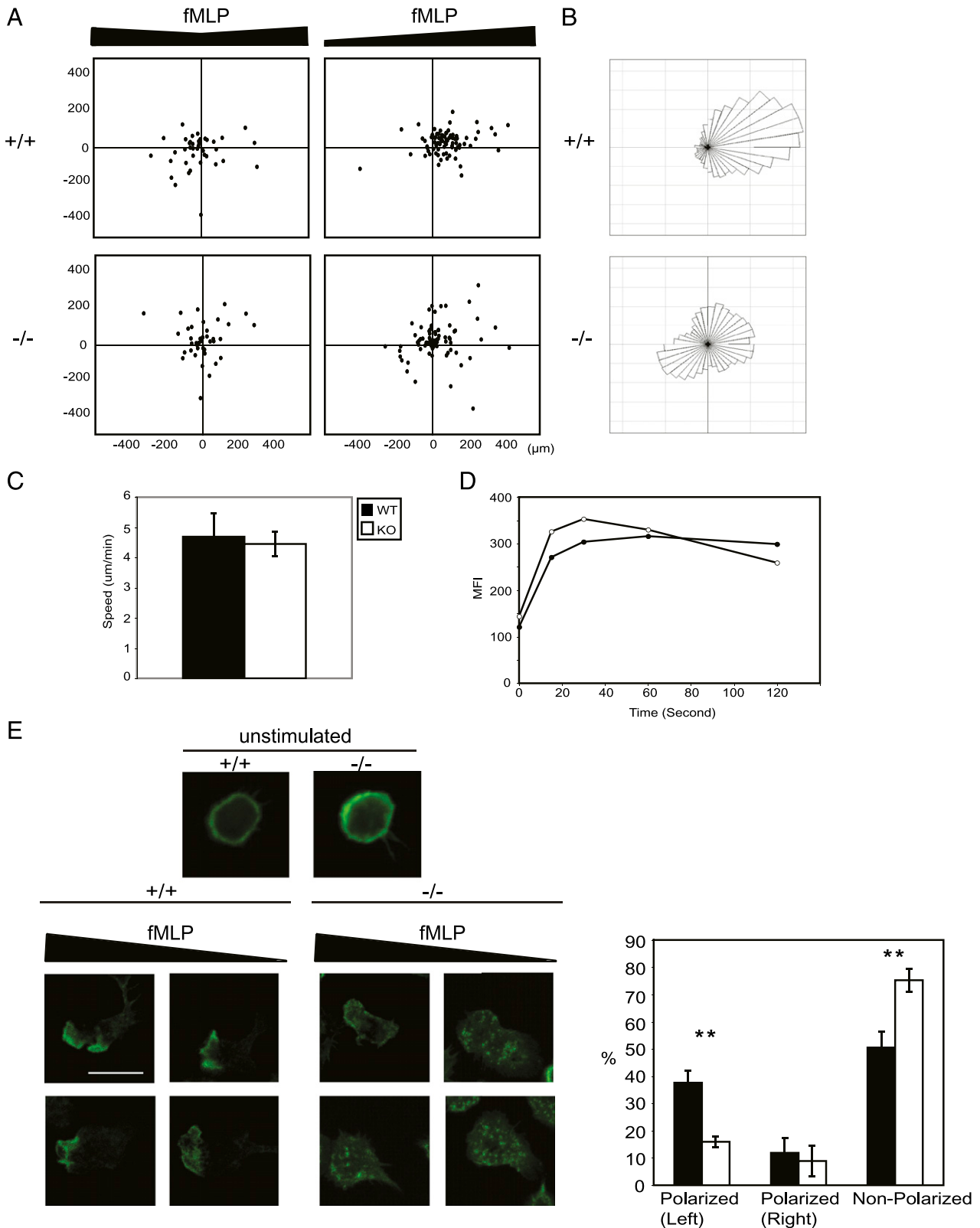


FIGURE 1. 3BP2 is required for neutrophil chemotaxis and spatially restricted F-actin assembly. **(A)** Plots of neutrophil migration in the Zigmond chamber assay are shown. Neutrophils undergoing chemokinesis (*left panels*) and chemotaxis (*right panels*) in response to fMLP were recorded using time-lapse imaging. Tracings were used to plot the final position of cells after 30 min. Each datum point on the plot represents one individual cell. The diagrams shown contain the combined traces from three independent experiments. The final positions of *Sh3bp2*^{+/+} and *Sh3bp2*^{-/-} neutrophils were subjected to the Rayleigh test of uniformity (*p* value of 3.76×10^{-12} for *Sh3bp2*^{+/+} cells and *p* value of 0.87 for *Sh3bp2*^{-/-} cells). **(B)** Rose diagram of cell tracks shown in **(A)**. **(C)** Average speeds (means \pm SEM) of all chemotaxing *Sh3bp2*^{+/+} (filled bar) and *Sh3bp2*^{-/-} (open bar) neutrophils in **(A)**. **(D)** A representative plot of FACS analysis of fMLP-stimulated total F-actin generation of *Sh3bp2*^{+/+} (●) and *Sh3bp2*^{-/-} (○) neutrophils is shown. Freshly isolated BM neutrophils were stimulated with 10 μM fMLP for the indicated time and analyzed for the content of F-actin by staining the cells with phalloidin. The results are expressed as the mean channel fluorescence. The plot is representative of three separate (*Figure legend continues*)

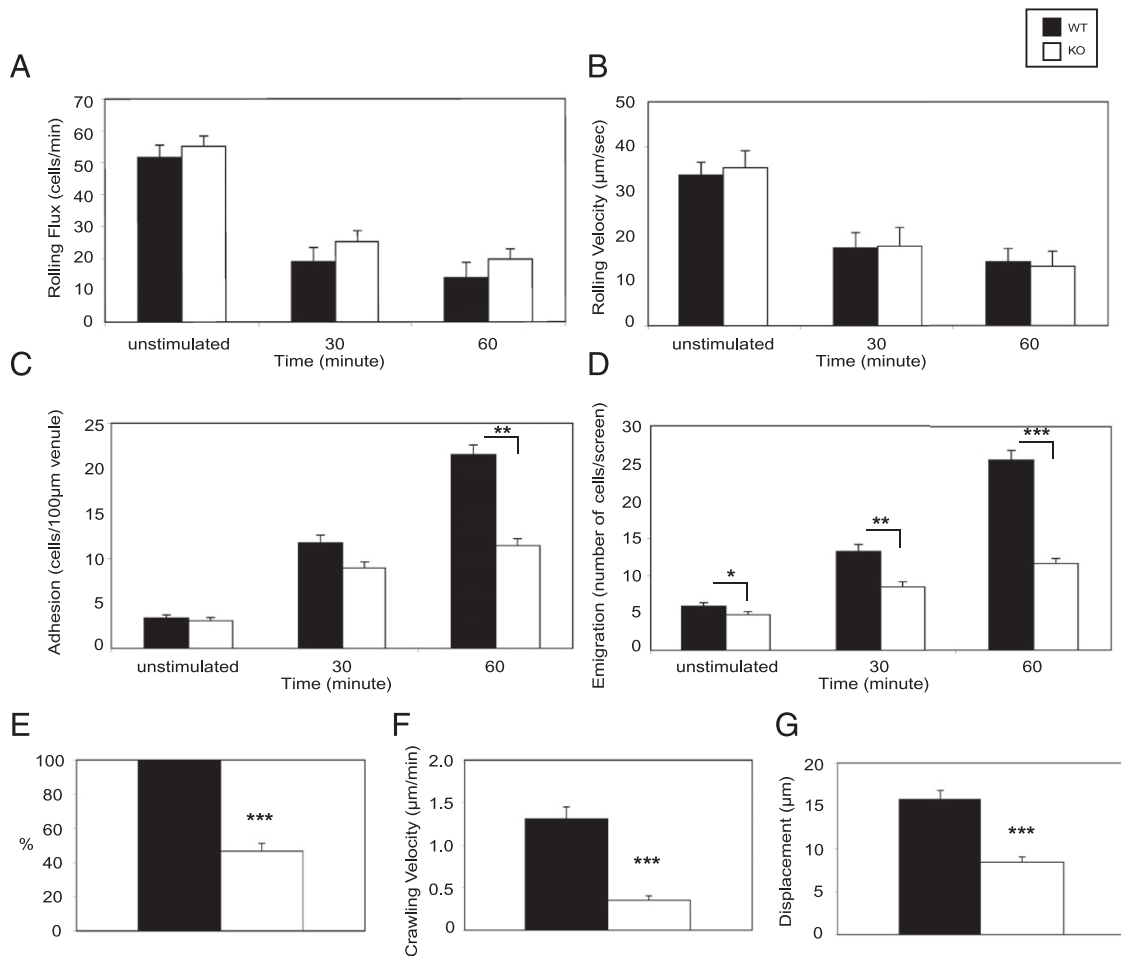


FIGURE 2. The role of 3BP2 in leukocyte recruitment and crawling in response to fMLF *in vivo*. Rolling flux (**A**), rolling velocity (**B**), adhesion (**C**), and emigration (**D**) of leukocytes before and after superfusion of fMLF (0.5 μM). All values are means of $n = 5 \pm$ SEM. (**E**) The percentage of adherent cells that crawled prior to emigrating out of the vessel in *Sh3bp2*^{+/+} (filled bar) and *Sh3bp2*^{-/-} mice (open bar). (**F**) The crawling velocity of adherent *Sh3bp2*^{+/+} (filled bar) and *Sh3bp2*^{-/-} (open bar) neutrophils. (**G**) The distance crawled by a *Sh3bp2*^{+/+} (filled bar) and *Sh3bp2*^{-/-} (open bar) neutrophils from the point of adhesion to where the emigration took place. All values are means of $n = 4 \pm$ SEM. * $p < 0.05$, ** $p < 0.01$, *** $p < 0.001$ compared with *Sh3bp2*^{+/+} mice.

wild-type neutrophils either into wild-type control mice or into *Sh3bp2*^{-/-} mice and quantified the number of Gr-1⁺ neutrophils recruited into peritoneal cavity following thioglycolate-induced peritonitis (Supplemental Fig. 1B, 1C). We observed a significant defect in neutrophil recruitment into peritoneal cavity of the 3BP2-deficient host mice compared with the wild-type controls ($1 \pm 0.3 \times 10^4$ cells in *Sh3bp2*^{-/-} recipient mice compared with $2.7 \pm 0.6 \times 10^4$ cells in wild-type recipient mice; Supplemental Fig. 1C). These data revealed a role of 3BP2 in the maintenance of the endothelial barrier regulating neutrophil recruitment into inflammatory sites. We have shown that the *in vivo* migratory defect of *Sh3bp2*^{-/-} neutrophils resulted from the combined effects of 3BP2 in both the neutrophil and endothelial cell compartments.

Superoxide production is reduced in *Sh3bp2*^{-/-} neutrophils

Neutrophils produce superoxide anions rapidly after exposure to proinflammatory mediators such as complement fragment C5a and *N*-formylmethionyl oligopeptides (41). We examined the effect of 3BP2 deficiency on fMLF-induced production of superoxide in

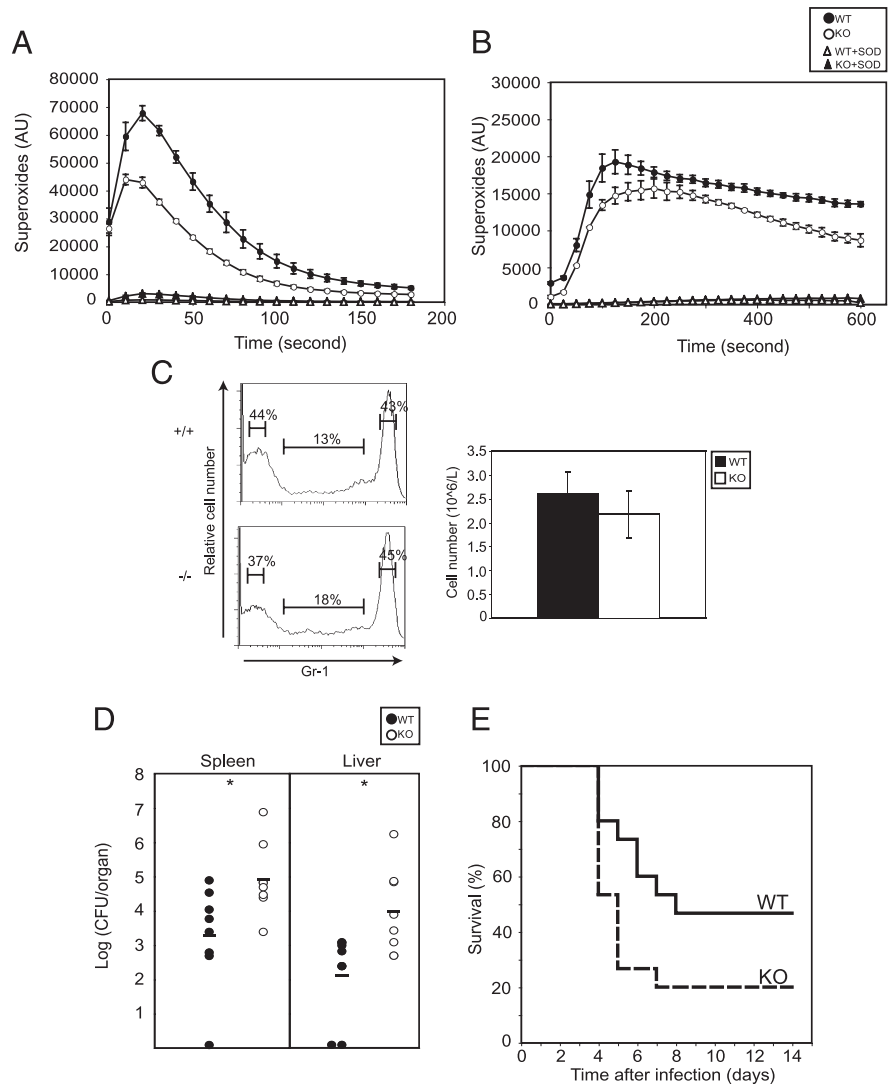
primary neutrophils. Both *Sh3bp2*^{+/+} and *Sh3bp2*^{-/-} neutrophils produced superoxide following fMLF stimulation that was quenched by superoxide dismutase. The kinetics of superoxide production were similar between both strains of mice. However, compared with *Sh3bp2*^{+/+} cells at 30 s following fMLF stimulation, *Sh3bp2*^{-/-} neutrophils produced 36% less superoxide anions (Fig. 3A). Phorbol ester-stimulated superoxide production was modestly but consistently lower in *Sh3bp2*^{-/-} neutrophils (Fig. 3B). Based on these results, we concluded that 3BP2 is involved in both chemoattractant- and PMA-induced superoxide production.

Increased susceptibility of *Sh3bp2*^{-/-} mice to *L. monocytogenes* infection

Both functional neutrophils and the fMLF receptor (formyl peptide receptor) are required for efficient clearance of *L. monocytogenes* infection (42–45). Given the defects in fMLF-induced chemotaxis, vascular emigration, and superoxide production that we observed in the *Sh3bp2*^{-/-} neutrophils, we next tested whether 3BP2-deficient mice might have reduced capacity to clear bacterial infections.

experiments with a consistent pattern. (**E**) Neutrophil chemotaxing under an fMLF gradient were stained with phalloidin and the percentages of *Sh3bp2*^{+/+} (filled bar) and *Sh3bp2*^{-/-} (open bar) neutrophils with polarized F-actin structures were compared. Results presented are average numbers from three independent experiments (means \pm SEM) (500 cells were counted per genotype per experiment, ** $p < 0.01$). Cells were judged to have polarized F-actin when F-actin staining is confined to less than one third of the circumference. Scale bar, 10 μm.

FIGURE 3. Effect of 3BP2 deficiency on superoxide production and antilisterial host defense. *Sh3bp2*^{+/+} (●) and *Sh3bp2*^{-/-} (○) neutrophils were stimulated with 10 μM fMLF for 3 min (A) or stimulated with 1 μM PMA for 10 min (B). Kinetic plots of chemiluminescence intensity are shown. The plots presented are representative of three individual experiments. Each point is the mean of three individual measurements, and the error bars are the SD of triplicate readings. (C) *Sh3bp2*^{+/+} and *Sh3bp2*^{-/-} BM cells were stained with PE-anti-Gr-1 Ab to determine the percentage of Gr-1-positive cells. The plots presented are representative of three individual experiments. Blood was collected from 9- to 11-wk-old *Sh3bp2*^{+/+} and *Sh3bp2*^{-/-} mice, and the absolute number of blood circulating neutrophils was determined using a Hemavet 950 (Drew Scientific Group) by the Toronto Center for Phenogenomics ($n = 6$ in each group; $p = 0.155$). (D) Nine- to 11-wk-old *Sh3bp2*^{+/+} (●) and *Sh3bp2*^{-/-} (○) mice were injected with 2×10^4 CFU *L. monocytogenes* in the tail vein. The bacterial burden from whole spleen and liver was determined 2 d after infection. Results presented are from a single experiment with sex-matched mice ($n = 8$ in each group) and are representative of three separate experiments with a consistent pattern. The mean values are indicated as solid bars. * $p < 0.05$, Mann-Whitney U test. (E) Nine- to 11-wk-old *Sh3bp2*^{+/+} (●) and *Sh3bp2*^{-/-} (○) mice were injected with 10^5 CFU *L. monocytogenes* in the tail vein. The percentage of death in the two groups was recorded for the duration of 14 d. Results presented are the combined results from three independent experiments with sex-matched mice ($n = 15$ in each group; $p = 0.0404$, Gehan-Breslow-Wilcoxon test).



3BP2 is not required for maintaining the steady-state levels of neutrophils, as both *Sh3bp2*^{+/+} and *Sh3bp2*^{-/-} mice had a similar percentage of Gr-1⁺ cells in their BM and comparable numbers of neutrophils in circulation (Fig. 3C). To test the role of 3BP2 in host defense, we compared the susceptibility of *Sh3bp2*^{+/+} and *Sh3bp2*^{-/-} mice to infection with *L. monocytogenes*. We infected mice with 2×10^4 CFU *L. monocytogenes* and measured the bacterial burden 2 d later, a time interval when the innate immune response is principally responsible for infection control (45). Relative to wild-type control mice, *Sh3bp2*^{-/-} mice carried 47- and 76-fold more bacteria in spleen and liver, respectively (Fig. 3D). We next tested the resistance of *Sh3bp2*^{-/-} mice to a higher bacterial burden of *L. monocytogenes* infection. Mice were challenged with 10^5 CFU bacteria and then analyzed 4–8 d later. After the first 4 d, 80% of wild-type mice were alive compared with 53% survival of the *Sh3bp2*^{-/-} mice cohort. By the day 8 after infection, 47% of *Sh3bp2*^{+/+} mice were alive whereas only 20% of *Sh3bp2*^{-/-} mice had survived (Fig. 3E). The results from both the bacterial burden assay and the survival assay demonstrated that 3BP2 is required for mice to mount an effective host defense against *Listeria* infection.

3BP2 is required for activation of Src family kinases and Rac2 GTPase

We have demonstrated that 3BP2 is required for fMLF-mediated neutrophil chemotaxis in vitro and in vivo and for maximal ROS

production in vitro. To determine what signaling events downstream of fMLF require 3BP2, we interrogated the signal transduction pathways activated in response to fMLF in both wild-type and *Sh3bp2*^{-/-} neutrophils. Neutrophil stimulation by fMLF results in acute tyrosine phosphorylation of several proteins, including one species with a molecular mass of 80 kDa, which may correspond to 3BP2 (46, 47). We examined 3BP2 tyrosine phosphorylation in response to fMLF and found that it is acutely tyrosine phosphorylated following fMLF stimulation (Fig. 4A). Src tyrosine kinases have been identified as downstream effectors of formyl peptide receptor signaling (16) and may regulate neutrophil integrin function (48, 49). Because we have previously demonstrated that 3BP2 binds to Src kinase and is required for integrin-mediated Src activation in osteoclasts (36), we examined 3BP2 dependency of Src activation in response to fMLF in neutrophils. We found that in the absence of 3BP2, the basal level of Src phosphorylation was reduced by 25% and the levels of fMLF-induced Src phosphorylation were diminished by 40% at 10 s and 50% at 40 s following stimulation compared with wild-type neutrophils (Fig. 4B).

The small GTPases Rac1 (20, 21, 50), Rac2 (19, 28, 50), and Cdc42 (23, 25) are known to be key regulators of the actin cytoskeleton whereas Rac2 is uniquely critical for activating the NADPH oxidase system in neutrophils (19, 27, 28). We assessed the levels of active Rac1, Rac2, and Cdc42 following fMLF

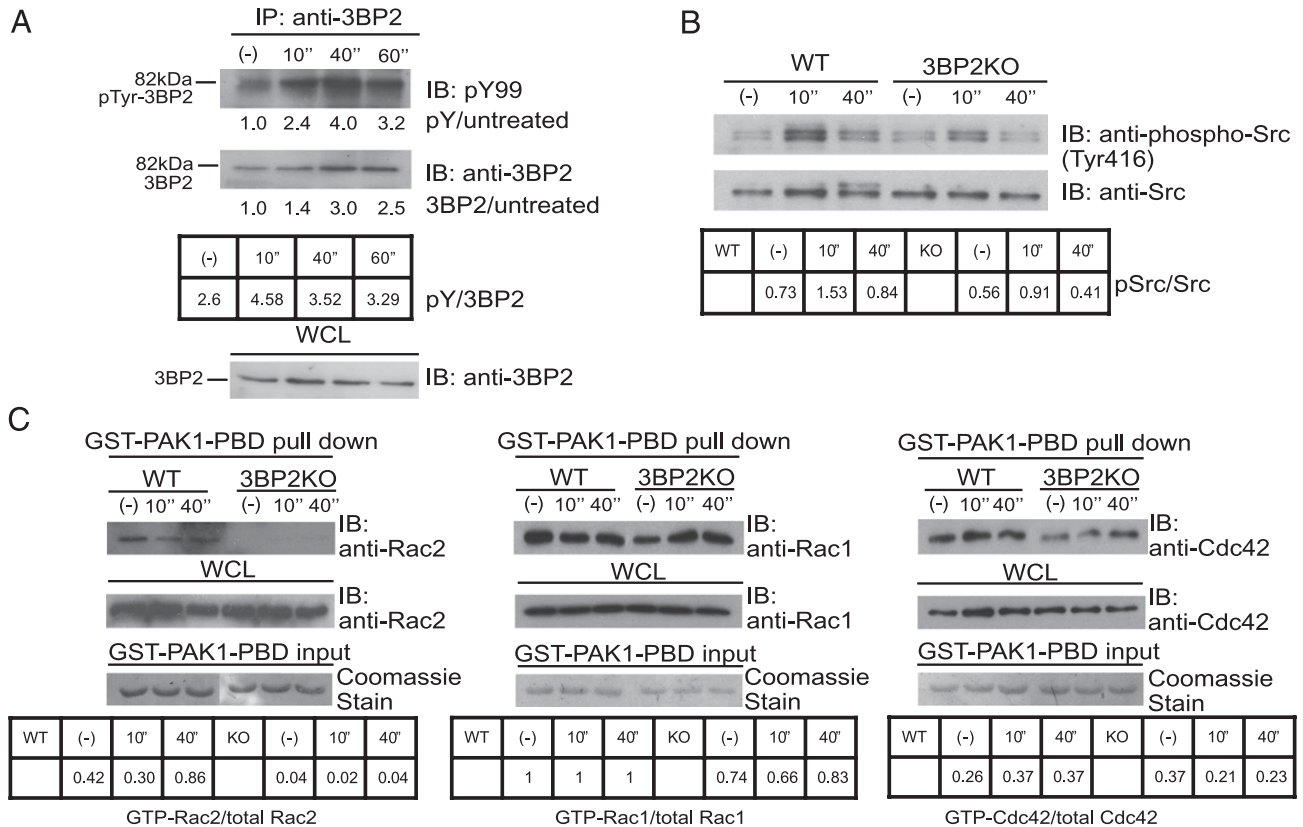


FIGURE 4. 3BP2 is tyrosine phosphorylated and is required for Src kinases and Rac2 GTPase activation. **(A)** Resting *Sh3bp2*^{+/+} BM neutrophils were either left unstimulated or stimulated with 10 μ M fMLF for indicated time intervals at 37°C before lysis. 3BP2 was immunoprecipitated, resolved by SDS-PAGE, and probed with anti-phosphotyrosine Ab, pY99, and the same membrane was stripped and reprobed with anti-3BP2. **(B)** Cell lysates from unstimulated and 10 μ M fMLF-stimulated *Sh3bp2*^{+/+} and *Sh3bp2*^{-/-} neutrophils were resolved by SDS-PAGE gel and probed with a phosphospecific Ab against phospho-Src. The same membrane was stripped and reprobed with an anti-Src Ab. **(C)** The levels of active Rac2 (left panel), Rac1 (middle panel), and Cdc42 (right panel) were determined in 10 μ M fMLF-stimulated BM neutrophils via the GST-PBD pull-down assay.

stimulation using the GTPase binding domain from Pak1 as an affinity reagent. In wild-type neutrophils, both Rac1 and Rac2 were GTP bound with little further induction of the GTP-bound state in response to fMLF. In *Sh3bp2*^{-/-} neutrophils we detected a significant reduction in Rac2 activation, whereas Rac1 activation was unaffected in these cells (Fig. 4C, left and middle panels). Additionally, we observed that the activation of Cdc42 was diminished in the absence of 3BP2 (Fig. 4C, right panel). Our data show that 3BP2 is required for the specific activation of Rac2 and the optimal activation of Cdc42 but has little impact on Rac1-GTP loading.

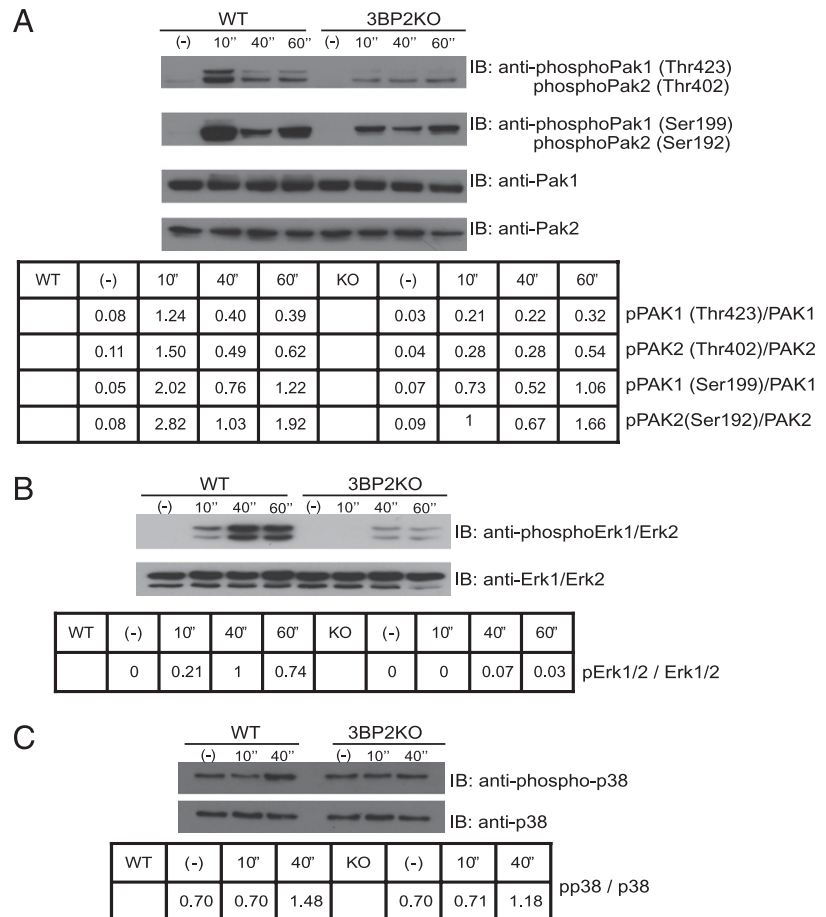
3BP2 is required for p21-activated protein kinase activation and MAPK activation in response to fMLF stimulation

Rac and Cdc42 GTPases are potent activators of the p21-activated serine/threonine protein kinases (Paks) (51), and Paks are activated following fMLF stimulation in neutrophils (52, 53). Pak family kinases contain an N-terminal regulatory domain that is composed of the PBD overlapping with an autoinhibitory domain (54). Control of Pak kinase activity depends on both the N-terminal regulatory region and the state of phosphorylation of Thr⁴²³ in the kinase activation loop (55, 56). Crystal structure of Pak1 showed that it exists as a homodimer where the N-terminal regulatory domain of one Pak1 molecule binds and inhibits the C-terminal catalytic domain of the other (57, 58). The structural data (57, 59, 60) and biochemical studies (61, 62) support a model in which Rac and Cdc42 GTPase binding to the PBD of Pak disrupts dimerization and leads to a series of conformational changes that rearrange the kinase

active site of Pak into a catalytically competent state (57). Phosphorylation at Thr⁴²³ in the activation loop of Pak1 catalytic domain by phosphoinositide-dependent kinase-1 (63) is critical to reinforce the active catalytic state of Pak1 (56, 64). With a deficiency in both Rac2 and Cdc42 activities, we hypothesized that Pak would fail to be fully activated in the absence of 3BP2. To examine the requirement of 3BP2 for fMLF-mediated Pak activation, we used phospho-specific Abs against Pak1 phospho-Ser¹⁹⁹/Thr⁴²³ and Pak2 phospho-Ser¹⁹²/Thr⁴⁰² as surrogate indicators of their activation state following stimulation. We observed that whereas both Pak1 and Pak2 were acutely phosphorylated in wild-type neutrophils, phosphorylation of Pak1 and Pak2 was significantly diminished in the absence of 3BP2 (Fig. 5A).

Pak kinases have been implicated in the regulation of MAPKs (65–69), cytoskeletal dynamics (70–72), and activation of NADPH oxidase complex (52, 73). The MAPK Erk p42/p44 is one of the Pak substrates and is activated in neutrophils following chemoattractant stimulation (19, 74, 75). Erk p42/p44 phosphorylation of p47^{phox}, one of the cytosolic components of the NADPH oxidase complex (76), is thought to be functionally important because selective MAPK pharmacologic inhibitors block fMLF-mediated superoxide production in neutrophils (77–79). The role of p38 MAPK in fMLF-mediated respiratory burst, in contrast, remains controversial (76, 80). We examined the phosphorylation of these MAPKs in response to fMLF to assess whether their activation was defective in the absence of 3BP2. We found that phosphorylation of Erk p42/p44 MAPK was significantly diminished in *Sh3bp2*^{-/-} neutrophils compared with wild-type neutrophils (Fig.

FIGURE 5. 3BP2 is required for the full activation of Pak1/2 kinase and Erk1/2 MAPK but not p38 MAPK. **(A)** Cell lysates from unstimulated and 10 μ M fMLF-stimulated *Sh3bp2*^{+/+} and *Sh3bp2*^{-/-} BM neutrophils were resolved by SDS-PAGE gel and probed with phospho-specific Abs against phospho-Pak1/2 (Thr⁴²³/Thr⁴⁰²) and phospho-Pak1/2 (Ser¹⁹⁹/Ser¹⁹²). The levels of Pak1/2 proteins were examined using anti-Pak1 and anti-Pak2. **(B)** Cell lysates were prepared as described above and a phospho-specific Ab against phospho-Erk1/2 was used to compare the levels of phospho-Erk1/2 in *Sh3bp2*^{+/+} and *Sh3bp2*^{-/-} BM neutrophils. The same membrane was stripped and reprobed with anti-Erk1/2. **(C)** Cell lysates were prepared as described above and a phospho-specific Ab against phospho-p38 was used to compare the levels of phospho-p38 in *Sh3bp2*^{+/+} and *Sh3bp2*^{-/-} BM neutrophils. The same membrane was stripped and reprobed with anti-p38.



5B), whereas no difference in the phosphorylation state of p38 MAPK was observed between *Sh3bp2*^{+/+} and *Sh3bp2*^{-/-} neutrophils (Fig. 5C). These results closely resemble the biochemical defects observed in fMLF-stimulated *Rac2*^{-/-} neutrophils (19), suggesting that *Rac2* is a major downstream component of the 3BP2 pathway in neutrophils.

3BP2 is required for the tyrosine phosphorylation of GEF Vav1 and the localization of GEF P-Rex1 to the leading edge in response to fMLF stimulation

Several Rac GEFs, including Vav (81, 82), GIT2 (30), and P-Rex1 (83, 84), are required for full fMLF response in neutrophils. Vav1 undergoes Src family kinase-dependent tyrosine phosphorylation in murine neutrophils stimulated with fMLF (82). Functionally, Vav1 participates in fMLF-induced neutrophil migration, F-actin polymerization, and superoxide production (82). Vav1 interacts with p67^{phox}, a target of Rac-GTP in the oxidase complex (85, 86), which enhances superoxide production by increasing nucleotide exchange on Rac (87). This localized pool of Rac2-GTP seems to be small, as the overall cellular level of Rac2-GTP induced by fMLF stimulation was not reduced in the absence of Vav1 (82). The attenuation in fMLF-induced superoxide production found in *Sh3bp2*^{-/-} neutrophils prompted us to examine Vav1 activation in these cells. We found that 3BP2 constitutively bound to Vav1 in neutrophils (Fig. 6A). The induction of Vav1 tyrosine phosphorylation was significantly reduced in the absence of 3BP2 after 1 min fMLF stimulation compared with wild-type neutrophils (Fig. 6B). Because we observed a substantial decrease in the overall levels of Rac2-GTP in *Sh3bp2*^{-/-} neutrophils (Fig. 4C), we conjectured that 3BP2 deficiency most likely is required for the function of other GEFs in neutrophils.

P-Rex1-deficient neutrophils demonstrated a differential effect on Rac2 compared with Rac1 activation in response to fMLF (84). Moreover, P-Rex1 is required for neutrophil migration rate and superoxide production in response to fMLF (31, 84). P-Rex1 polarizes to the leading edge of neutrophils during chemotaxis in a region where phosphatidylinositol 3,4,5-trisphosphate (PIP₃) accumulates following activation of class I PI3K (26, 88, 89). P-Rex1 activation requires the coincident input of PIP₃ phospholipids and G β γ dimers (83), suggesting that its localization in proximity to these two agonists at the leading edge may be a requirement for its full activation. Because *Sh3bp2*^{-/-} neutrophils closely phenocopied the biologic defects observed in *P-Rex1*^{-/-} neutrophils, we investigated the possibility that 3BP2 and P-Rex1 are functionally coupled. We were unable to demonstrate an endogenous 3BP2/P-Rex1 protein complex in neutrophils, nor were we able to show that the levels of P-Rex1 tyrosine phosphorylation were altered in 3BP2-deficient neutrophils (data not shown). We next examined the subcellular localization of P-Rex1 in neutrophils under basal conditions and in an fMLF gradient. Under basal conditions, P-Rex1 was distributed in a nonpolarized uniform manner in both *Sh3bp2*^{+/+} and *Sh3bp2*^{-/-} neutrophils. In response to an fMLF gradient, we observed that P-Rex1 moved to the leading edge of the cell in ~40% of wild-type neutrophils undergoing chemotaxis. In comparison, only ~14% of *Sh3bp2*^{-/-} neutrophils displayed a polarized P-Rex1 distribution when exposed to an fMLF gradient (Fig. 6C). The failure of P-Rex1 localization was not due to lack of PI3K activation and PIP₃ production because the phosphorylation of Akt was not reduced in the absence of 3BP2 (Fig. 6D). Our results demonstrate a requirement for 3BP2 in specifying the leading edge polarization of P-Rex1 during neutrophil chemotaxis and suggest that this defect may be

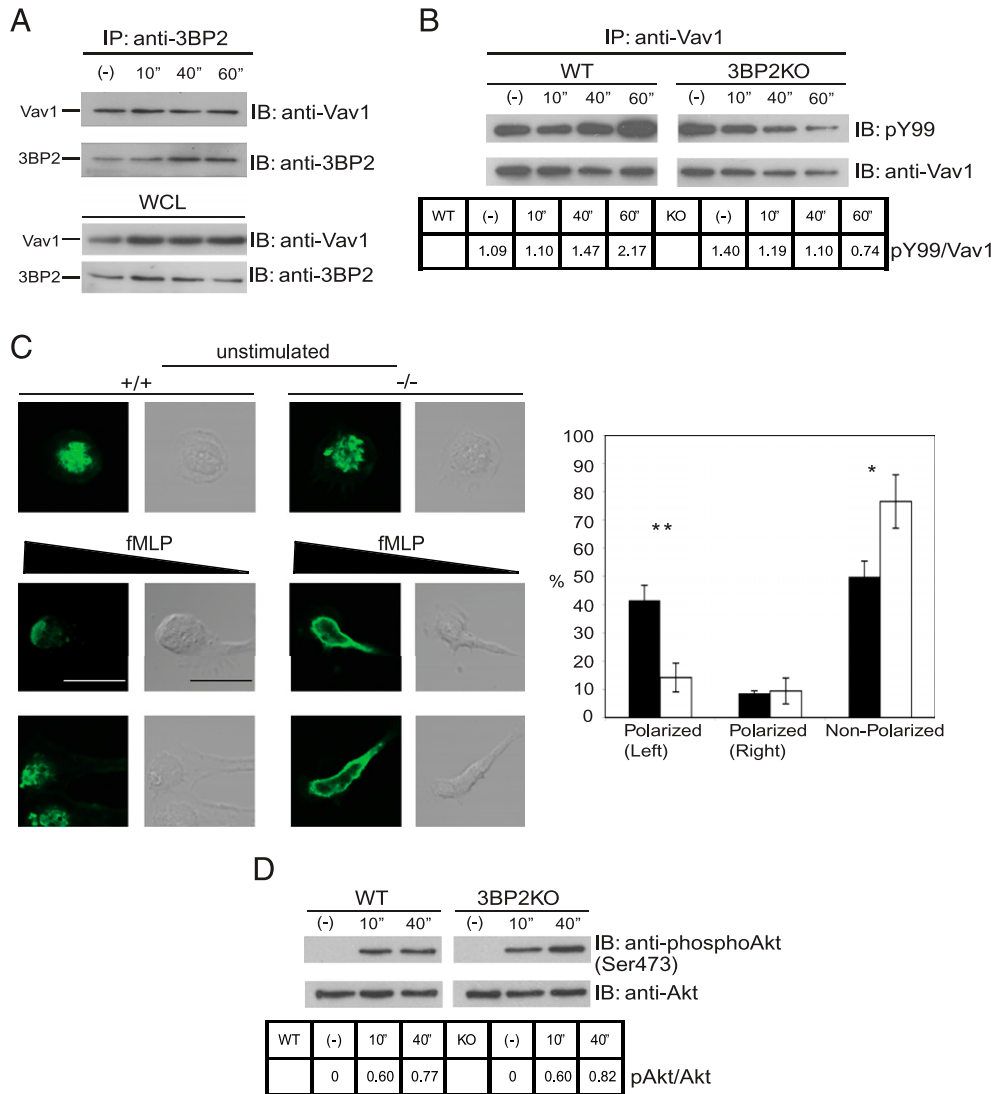


FIGURE 6. 3BP2 constitutively binds to Vav1 and is required for Vav1 tyrosine phosphorylation and P-Rex1 localization following fMLF stimulation. **(A)** Resting *Sh3bp2*^{+/+} neutrophils were either left unstimulated or stimulated with 10 μ M fMLF for indicated time intervals at 37°C before lysis. 3BP2 was immunoprecipitated, resolved by SDS-PAGE, and probed with anti-Vav1 Ab. The same membrane was stripped and reprobed with anti-3BP2. **(B)** Kinetics and magnitude of immunoprecipitated Vav1 tyrosine phosphorylation following fMLF stimulation were compared between *Sh3bp2*^{+/+} and *Sh3bp2*^{-/-} neutrophils. **(C)** Neutrophil chemotaxis under an fMLF gradient were stained with anti-P-Rex1 mAb as described in *Materials and Methods*. The data shown here contained both immunofluorescence image (*left side*) and differential interference contrast image (*right side*) of the same cell. The percentages of *Sh3bp2*^{+/+} (filled bar) and *Sh3bp2*^{-/-} (open bar) neutrophils with asymmetrical accumulation of P-Rex1 were compared. Scale bars, 10 μ m. Results presented are average numbers from three independent experiments (mean \pm SEM) (~1000 cells were counted per genotype per experiment, **p* < 0.05, ***p* < 0.01). **(D)** Cell lysates from unstimulated and 10 μ M fMLF-stimulated *Sh3bp2*^{+/+} and *Sh3bp2*^{-/-} neutrophils were resolved by SDS-PAGE gel and probed with a phospho-specific Ab against phospho-Akt. The same membrane was stripped and reprobed with anti-Akt.

related to the failure of Rac2 to become activated in the absence of 3BP2.

Discussion

In this study, we report the requirement for the pleckstrin homology/Src homology 2-containing adapter protein 3BP2 for optimal neutrophil function both in vitro and in vivo. Mice lacking 3BP2 are unable to mount an effective response to acute *L. monocytogenes* infection, and neutrophils from these mice are defective in intravascular crawling and endothelial emigration in response to fMLF in vivo. The inability of *Sh3bp2*^{-/-} neutrophils to respond to fMLF in vivo is mirrored by their inability to undergo productive chemotaxis in response to an fMLF gradient in vitro. Moreover, neutrophils lacking 3BP2 fail to polarize their polymerized actin cytoskeleton toward the fMLF gradient, an obligate step

during chemotaxis. We also observed that *Sh3bp2*^{-/-} neutrophils were unable to generate normal ROS levels in response to fMLF in vitro. These observations provide genetic evidence that 3BP2 couples fMLF signaling to the actin cytoskeleton reorganization during chemotaxis and to the NADPH oxidase complex.

fMLF signals through a GPCR system, which recruits lipid kinases, protein kinases, GEFs, and small GTPases (17). In this study, we show that 3BP2 adapter protein is required in neutrophils for maximal Src family kinase activation and is itself rapidly tyrosine phosphorylated following fMLF stimulation. The most profound signaling defect we observed in the 3BP2-deficient neutrophils was attenuated Rac2 activation in the context of normal Rac1 activation in response to fMLF. This defect manifested a phenotype reminiscent of *Rac2*^{-/-} neutrophils, including decreased superoxide production (27), defective directed migration

(19), and poor F-actin polarization (28). These observations suggest that 3BP2 and Rac2 may share a common biochemical pathway. In distinction to Rac1, Rac2 exists in at least two distinct functional and spatially resolved pools in neutrophils (28). Rac2 is enriched in a perinuclear pool critical for activation of the NADPH oxidase complex (27, 28, 86) and in regions interior to but distinct from cortical F-actin within the lamellipodium required for pseudopodium formation and cell polarization in response to fMLF stimulation (28). The C-terminal prenylation sequence of Rac2, RQKRP, is both necessary and sufficient for directing Rac2 to the perinuclear region and is indispensable for Rac2-mediated superoxide production in neutrophils (28), whereas the RQKRP sequence together with aspartic acid at position 150 are both required for localization to the cytoplasm associated with F-actin polarization and directed migration (28). Although Rac1-GTP cannot compensate for Rac2-dependent superoxide production in the absence of Rac2, replacement of the C-terminal sequence of Rac1 with the RQKRP sequence derived from Rac2 is sufficient to restore the superoxide production in Rac2^{-/-} neutrophils (28). These distinct pools of Rac2 may be regulated by distinct guanine nucleotide exchange factors. We show that Vav1 is a 3BP2-binding partner in neutrophils. Vav1 forms an fMLF-inducible complex with p67^{phox} and Rac2 in human neutrophils (87). The kinetics of this association are similar to the kinetics of superoxide formation elicited by fMLF (87), suggesting that Vav1 is the principal GEF that controls the activation of the perinuclear pool of Rac2 responsible for neutrophil ROS production. The restricted regulation of the perinuclear Rac2 pool by Vav1 may explain, in part, the paradox that whereas the overall cellular Rac2-GTP levels are near normal in Vav1^{-/-} neutrophils, the superoxide production is reduced 3-fold in these cells in response to fMLF (82). Consistent with the defect in superoxide production observed in *Sh3bp2*^{-/-} neutrophils, we observed a significant reduction in Vav1 phosphorylation in the absence of 3BP2 in response to fMLF.

Our data demonstrating a severe reduction in total Rac2-GTP in *Sh3bp2*^{-/-} neutrophils suggest that 3BP2 regulates the activity of other Rac GEFs in addition to Vav. The selective Rac2-GTP loading defect in the absence of altered Rac1-GTP levels in *Sh3bp2*^{-/-} neutrophils closely phenocopies a similar defect observed in the P-Rex1-deficient neutrophils (31). Although we were unable to demonstrate an inducible 3BP2/P-Rex1 protein complex in neutrophils or show that P-Rex1 tyrosine phosphorylation levels were dependent on 3BP2, we observed that 3BP2 is required for polarization of P-Rex1 to the leading edge of cells migrating in an fMLF gradient. P-Rex1 activation is dependent on both Gβγ dimers and the PI3K lipid product PIP₃ (83). The precise mechanism of how Gβγ subunits and PIP₃ activate P-Rex1 is currently unknown. One model suggests that the Gβγ subunits and PIP₃ lipids bind to and activate P-Rex1 by inducing an allosteric reorganization of its GEF catalytic domain (83). In chemoattractant-stimulated neutrophils, PIP₃ accumulates asymmetrically at the leading edge of the cell as a result of local accumulation of active PI3K in this region (22). The confinement of PIP₃ to the inner leaflet of the leading edge of the cell (26, 88) serves to activate P-Rex1 and hence Rac2 in a temporally and spatially restricted manner (90). We have shown that in wild-type neutrophils, P-Rex1 accumulates at the leading edge in a region where PIP₃ and active Rac levels are known to be elevated (88, 90–92). In the absence of 3BP2, P-Rex1 fails to localize to the leading edge, which suggests that this localization defect could therefore uncouple P-Rex1 from PIP₃-mediated activation and subsequent efficient Rac2-GTP loading (31).

In addition to defects in superoxide generation, neutrophils deficient in Rac2 are incapable of polarization of polymerized actin

(28) required for chemotaxis (19). The redistribution of Rac2 interior to F-actin in response to fMLF is required to mediate F-actin polarization and chemoattractant-induced cell migration in neutrophils (28). Genetic analyses of Vav1^{-/-} (82) and P-Rex1^{-/-} neutrophil Rac-GTP loading (31, 84) suggest that whereas Vav1 is involved in activation of perinuclear Rac2 responsible for superoxide generation, P-Rex1 may control the activation of global Rac2 activation. The failure of P-Rex1 polarization to the leading edge might contribute to the quantitative deficiency in Rac2-GTP levels observed in *Sh3bp2*^{-/-} neutrophils and the defects in chemotaxis and superoxide production observed in these cells.

More recently, P-Rex1 and Vav1 have been shown to cooperate in the regulation of fMLF-dependent neutrophil response (93). Neutrophils lacking both P-Rex1 and Vav1 have severe defects in fMLF-dependent ROS formation, chemotaxis, and adhesion, whereas these responses are normal or near normal in cells lacking the entire P-Rex family or the entire Vav family (93). These observations further confirmed the role of 3BP2 in the activation of different GEFs downstream of the fMLF receptor. Because these two GEFs are activated through separate pathways downstream of the fMLF receptor, that is, P-Rex1 is targeted by Gβγ and PIP₃ (83), whereas Vav1 is activated by protein tyrosine kinase (82), 3BP2 is most likely involved in both signaling pathways.

In concert with the Rac2 defect we observed a severe defect in the activation of Rac/Cdc42 downstream kinases Pak1 and Pak2. Interestingly, Pak1 has a dual role of being an effector of Cdc42 and a stimulator for Cdc42 activation (25). A requirement for Pak1 in chemoattractant-induced Cdc42 activation and chemotaxis of cells was demonstrated using small interfering RNA-mediated Pak1 mRNA knockdown in RAW274 macrophage-like cell line and in differentiated HL-60 cells (25). Cdc42 controls cellular polarization and directional sensing (25, 94–97). The lack of optimal levels of Cdc42-GTP in *Sh3bp2*^{-/-} neutrophils therefore might also contribute to the chemotaxis defects observed in these cells.

The in vivo data presented in this study show that 3BP2 is required for neutrophil intraluminal crawling to optimal sites of emigration. Whereas all wild-type neutrophils that adhered to the venule wall immediately began crawling, neutrophils lacking 3BP2 were significantly impaired in their ability to crawl, which in turn led to impaired emigration. Intraluminal crawling has previously been described as a means for neutrophils to reach optimal emigration sites following adhesion (98). We observed that the few *Sh3bp2*^{-/-} neutrophils that successfully emigrated out of the vasculature crawled much shorter distances and their crawling velocities were also decreased. These data indicate that cells lacking 3BP2 either had impaired engagement of integrins and other adhesion molecules or suffered from an inability to disengage adhesive mechanisms. Intraluminal neutrophil crawling requires β₂ integrin Mac-1 (α_Mβ₂, CD11b/CD18) and its ligand, ICAM-1, whereas β₂ integrin LFA-1 (α_Lβ₂, CD11a/CD18) is needed for neutrophil adhesion (98). The defect in *Sh3bp2*^{-/-} neutrophil emigration is reminiscent of, but is less severe than, the defects observed in neutrophils lacking the β₂ integrins Mac-1 or LFA-1 (98), suggesting that 3BP2 likely modulates integrin function and is required for optimum integrin-dependent adhesion and crawling. Most leukocyte integrins exist in a resting state until activated by stimuli (99). Activation of neutrophils by fMLF stimulation provides inside-out signals that activate their integrin receptors by increasing the adhesive activity of these integrins (100). The stimulation-dependent integrin activation prevents the spontaneous adhesion of circulating leukocytes to the blood vessel wall (101). The inside-out signaling initiated by GPCR activates integrin receptors through enhanced ligand affinity (102–105) and

clustering of integrins by changing their lateral surface motility to achieve increased avidity for the ligand (106, 107). fMLF activates β_2 integrins by increasing receptor avidity and binding affinity (100). The specific mechanism and molecular components involved in the inside-out signal from the fMLF receptor to β_2 integrin remain to be elucidated (108). β_2 integrin-mediated outside-in signaling, however, is known to require activation of the Src family kinases Fgr and Hck (48), Syk (109), and Vav GEFs (110). We speculate that 3BP2 is required to couple fMLF stimulation with β_2 integrin activation. However, 3BP2 may also be directly required for outside-in integrin signal transduction.

Lastly, we uncovered a previously unanticipated role of 3BP2 in regulating the integrity of the endothelial barrier controlling the recruitment of neutrophils into inflammatory sites. Further study will be required to fully elucidate the role of 3BP2 in endothelial cells.

We have identified a new component, the adapter protein 3BP2, to a pathway that couples fMLF stimulation to actin polarization and ROS production in neutrophils. The cellular defects observed in the absence of 3BP2 stem from the inability to activate Src family kinases, Vav1 GEF, and properly localize P-Rex1, which is needed for Rac2 activation and its downstream effector proteins. As a result, 3BP2-deficient neutrophils have difficulty getting to sites of infection and effectively manifesting an antimicrobial response to *L. monocytogenes* once a bacterial target is encountered.

Disclosures

The authors have no financial conflicts of interest.

References

- Simon, S. I., and C. E. Green. 2005. Molecular mechanics and dynamics of leukocyte recruitment during inflammation. *Annu. Rev. Biomed. Eng.* 7: 151–185.
- Vento, S., and F. Cainelli. 2003. Infections in patients with cancer undergoing chemotherapy: aetiology, prevention, and treatment. *Lancet Oncol.* 4: 595–604.
- Schiffmann, E., B. A. Corcoran, and S. M. Wahl. 1975. N-formylmethionyl peptides as chemoattractants for leucocytes. *Proc. Natl. Acad. Sci. USA* 72: 1059–1062.
- Baggiolini, M., and I. Clark-Lewis. 1992. Interleukin-8, a chemotactic and inflammatory cytokine. *FEBS Lett.* 307: 97–101.
- Fernandez, H. N., P. M. Henson, A. Otani, and T. E. Hugli. 1978. Chemotactic response to human C3a and C5a anaphylatoxins. I. Evaluation of C3a and C5a leukotaxis in vitro and under stimulated in vivo conditions. *J. Immunol.* 120: 109–115.
- Strathmann, M. P., and M. I. Simon. 1991. G α 12 and G α 13 subunits define a fourth class of G protein α subunits. *Proc. Natl. Acad. Sci. USA* 88: 5582–5586.
- Gilman, A. G. 1987. G proteins: transducers of receptor-generated signals. *Annu. Rev. Biochem.* 56: 615–649.
- Gomez-Cambronero, J., C. K. Huang, V. A. Bonak, E. Wang, J. E. Casnellie, T. Shiraiishi, and R. I. Sha'afi. 1989. Tyrosine phosphorylation in human neutrophil. *Biochem. Biophys. Res. Commun.* 162: 1478–1485.
- Rollet, E., A. C. Caon, C. J. Roberge, N. W. Liao, S. E. Malawista, S. R. McColl, and P. H. Naccache. 1994. Tyrosine phosphorylation in activated human neutrophils: comparison of the effects of different classes of agonists and identification of the signaling pathways involved. *J. Immunol.* 153: 353–363.
- Naccache, P. H., C. Gilbert, A. C. Caon, M. Gaudry, C. K. Huang, V. A. Bonak, K. Umezawa, and S. R. McColl. 1990. Selective inhibition of human neutrophil functional responsiveness by erbstatin, an inhibitor of tyrosine protein kinase. *Blood* 76: 2098–2104.
- Kusunoki, T., H. Higashi, S. Hosoi, D. Hata, K. Sugie, M. Mayumi, and H. Mikawa. 1992. Tyrosine phosphorylation and its possible role in superoxide production by human neutrophils stimulated with FMLP and IgG. *Biochem. Biophys. Res. Commun.* 183: 789–796.
- Gutkind, J. S., and K. C. Robbins. 1989. Translocation of the FGR protein-tyrosine kinase as a consequence of neutrophil activation. *Proc. Natl. Acad. Sci. USA* 86: 8783–8787.
- Ptasznik, A., A. Traynor-Kaplan, and G. M. Bokoch. 1995. G protein-coupled chemoattractant receptors regulate Lyn tyrosine kinase/Shc adapter protein signaling complexes. *J. Biol. Chem.* 270: 19969–19973.
- Gaudry, M., C. Gilbert, F. Barabé, P. E. Poubelle, and P. H. Naccache. 1995. Activation of Lyn is a common element of the stimulation of human neutrophils by soluble and particulate agonists. *Blood* 86: 3567–3574.
- Hanke, J. H., J. P. Gardner, R. L. Dow, P. S. Changelian, W. H. Brissette, E. J. Weringer, B. A. Pollock, and P. A. Connelly. 1996. Discovery of a novel, potent, and Src family-selective tyrosine kinase inhibitor: study of Lck- and FynT-dependent T cell activation. *J. Biol. Chem.* 271: 695–701.
- Fumagalli, L., H. Zhang, A. Baruzzi, C. A. Lowell, and G. Berton. 2007. The Src family kinases Hck and Fgr regulate neutrophil responses to N-formyl-methionyl-leucyl-phenylalanine. *J. Immunol.* 178: 3874–3885.
- Bokoch, G. M. 1995. Chemoattractant signaling and leukocyte activation. *Blood* 86: 1649–1660.
- Hall, A. 1998. G proteins and small GTPases: distant relatives keep in touch. *Science* 280: 2074–2075.
- Roberts, A. W., C. Kim, L. Zhen, J. B. Lowe, R. Kapur, B. Petryniak, A. Spaetti, J. D. Pollock, J. B. Borneo, G. B. Bradford, et al. 1999. Deficiency of the hematopoietic cell-specific Rho family GTPase Rac2 is characterized by abnormalities in neutrophil function and host defense. *Immunity* 10: 183–196.
- Glogauer, M., C. C. Marchal, F. Zhu, A. Worku, B. E. Clausen, I. Foerster, P. Marks, G. P. Downey, M. Dinauer, and D. J. Kwiatkowski. 2003. Rac1 deletion in mouse neutrophils has selective effects on neutrophil functions. *J. Immunol.* 170: 5652–5657.
- Sun, C. X., G. P. Downey, F. Zhu, A. L. Koh, H. Thang, and M. Glogauer. 2004. Rac1 is the small GTPase responsible for regulating the neutrophil chemotaxis compass. *Blood* 104: 3758–3765.
- Srinivasan, S., F. Wang, S. Glavas, A. Ott, F. Hofmann, K. Aktories, D. Kalman, and H. R. Bourne. 2003. Rac and Cdc42 play distinct roles in regulating PI (3,4,5)P₃ and polarity during neutrophil chemotaxis. *J. Cell Biol.* 160: 375–385.
- Ma, L., R. Rohatgi, and M. W. Kirschner. 1998. The Arp2/3 complex mediates actin polymerization induced by the small GTP-binding protein Cdc42. *Proc. Natl. Acad. Sci. USA* 95: 15362–15367.
- Wong, K., O. Pertz, K. Hahn, and H. Bourne. 2006. Neutrophil polarization: spatiotemporal dynamics of RhoA activity support a self-organizing mechanism. *Proc. Natl. Acad. Sci. USA* 103: 3639–3644.
- Li, Z., M. Hannigan, Z. Mo, B. Liu, W. Lu, Y. Wu, A. V. Smrcka, G. Wu, L. Li, M. Liu, et al. 2003. Directional sensing requires G β -mediated PAK1 and PI3 α -dependent activation of Cdc42. *Cell* 114: 215–227.
- Xu, J., F. Wang, A. Van Keymeulen, P. Herzmark, A. Straight, K. Kelly, Y. Takuwa, N. Sugimoto, T. Mitchison, and H. R. Bourne. 2003. Divergent signals and cytoskeletal assemblies regulate self-organizing polarity in neutrophils. *Cell* 114: 201–214.
- Li, S., A. Yamauchi, C. C. Marchal, J. K. Molitoris, L. A. Quilliam, and M. C. Dinauer. 2002. Chemoattractant-stimulated Rac activation in wild-type and Rac2-deficient murine neutrophils: preferential activation of Rac2 and Rac2 gene dosage effect on neutrophil functions. *J. Immunol.* 169: 5043–5051.
- Filippi, M. D., C. E. Harris, J. Meller, Y. Gu, Y. Zheng, and D. A. Williams. 2004. Localization of Rac2 via the C terminus and aspartic acid 150 specifies superoxide generation, actin polarity and chemotaxis in neutrophils. *Nat. Immunol.* 5: 744–751.
- Kunisaki, Y., A. Nishikimi, Y. Tanaka, R. Takii, M. Noda, A. Inayoshi, K. Watanabe, F. Sanematsu, T. Sasazuki, T. Sasaki, and Y. Fukui. 2006. DOCK2 is a Rac activator that regulates motility and polarity during neutrophil chemotaxis. *J. Cell Biol.* 174: 647–652.
- Mazaki, Y., S. Hashimoto, T. Tsujimura, M. Morishige, A. Hashimoto, K. Aritake, A. Yamada, J. M. Nam, H. Kiyonari, K. Nakao, and H. Sabe. 2006. Neutrophil direction sensing and superoxide production linked by the GTPase-activating protein GIT2. *Nat. Immunol.* 7: 724–731.
- Dong, X., Z. Mo, G. Bokoch, C. Guo, Z. Li, and D. Wu. 2005. P-Rex1 is a primary Rac2 guanine nucleotide exchange factor in mouse neutrophils. *Curr. Biol.* 15: 1874–1879.
- Cicchetti, P., B. J. Mayer, G. Thiel, and D. Baltimore. 1992. Identification of a protein that binds to the SH3 region of Abl and is similar to Bcr and GAP-rho. *Science* 257: 803–806.
- Deckert, M., S. Tartare-Deckert, J. Hernandez, R. Rottapel, and A. Altman. 1998. Adaptor function for the Syk kinases-interacting protein 3BP2 in IL-2 gene activation. *Immunity* 9: 595–605.
- Foucault, I., S. Le Bras, C. Charvet, C. Moon, A. Altman, and M. Deckert. 2005. The adaptor protein 3BP2 associates with VAV guanine nucleotide exchange factors to regulate NFAT activation by the B-cell antigen receptor. *Blood* 105: 1106–1113.
- Chen, G., I. D. Dimitriou, J. La Rose, S. Ilangumaran, W. C. Yeh, G. Doody, M. Turner, J. Gommerman, and R. Rottapel. 2007. The 3BP2 adapter protein is required for optimal B-cell activation and thymus-independent type 2 humoral response. *Mol. Cell Biol.* 27: 3109–3122.
- Levaot, N., P. D. Simoncic, I. D. Dimitriou, A. Scotter, J. La Rose, A. H. Ng, T. L. Willett, C. J. Wang, S. Janmohamed, M. Grynaps, et al. 2011. 3BP2-deficient mice are osteoporotic with impaired osteoblast and osteoclast functions. *J. Clin. Invest.* 121: 3244–3257.
- Lowell, C. A., L. Fumagalli, and G. Berton. 1996. Deficiency of Src family kinases p59/lck and p58c-fgr results in defective adhesion-dependent neutrophil functions. *J. Cell Biol.* 133: 895–910.
- Heit, B., L. Liu, P. Colarusso, K. D. Puri, and P. Kubes. 2008. PI3K accelerates, but is not required for, neutrophil chemotaxis to fMLP. *J. Cell Sci.* 121: 205–214.
- Condeelis, J. 1993. Life at the leading edge: the formation of cell protrusions. *Annu. Rev. Cell Biol.* 9: 411–444.
- Stossel, T. P. 1989. From signal to pseudopod: how cells control cytoplasmic actin assembly. *J. Biol. Chem.* 264: 18261–18264.
- Thelen, M., B. Dewald, and M. Baggiolini. 1993. Neutrophil signal transduction and activation of the respiratory burst. *Physiol. Rev.* 73: 797–821.

42. Gao, J. L., E. J. Lee, and P. M. Murphy. 1999. Impaired antibacterial host defense in mice lacking the *N*-formylpeptide receptor. *J. Exp. Med.* 189: 657–662.
43. Rakhmievich, A. L. 1995. Neutrophils are essential for resolution of primary and secondary infection with *Listeria monocytogenes*. *J. Leukoc. Biol.* 57: 827–831.
44. Zhan, Y., G. J. Lieschke, D. Grail, A. R. Dunn, and C. Cheers. 1998. Essential roles for granulocyte-macrophage colony-stimulating factor (GM-CSF) and G-CSF in the sustained hematopoietic response of *Listeria monocytogenes*-infected mice. *Blood* 91: 863–869.
45. Conlan, J. W., and R. J. North. 1994. Neutrophils are essential for early anti-*Listeria* defense in the liver, but not in the spleen or peritoneal cavity, as revealed by a granulocyte-depleting monoclonal antibody. *J. Exp. Med.* 179: 259–268.
46. Grinstein, S., and W. Furuya. 1992. Chemoattractant-induced tyrosine phosphorylation and activation of microtubule-associated protein kinase in human neutrophils. *J. Biol. Chem.* 267: 18122–18125.
47. Torres, M., F. L. Hall, and K. O'Neill. 1993. Stimulation of human neutrophils with formyl-methionyl-leucyl-phenylalanine induces tyrosine phosphorylation and activation of two distinct mitogen-activated protein-kinases. *J. Immunol.* 150: 1563–1577.
48. Giagulli, C., L. Ottoboni, E. Cavegion, B. Rossi, C. Lowell, G. Constantini, C. Laudanna, and G. Berton. 2006. The Src family kinases Hck and Fgr are dispensable for inside-out, chemoattractant-induced signaling regulating β_2 integrin affinity and valency in neutrophils, but are required for β_2 integrin-mediated outside-in signaling involved in sustained adhesion. *J. Immunol.* 177: 604–611.
49. Sarantos, M. R., H. Zhang, U. Y. Schaff, N. Dixit, H. N. Hayenga, C. A. Lowell, and S. I. Simon. 2008. Transmigration of neutrophils across inflamed endothelium is signaled through LFA-1 and Src family kinase. *J. Immunol.* 181: 8660–8669.
50. Sun, C. X., M. A. Magalhães, and M. Glogauer. 2007. Rac1 and Rac2 differentially regulate actin free barbed end formation downstream of the fMLP receptor. *J. Cell Biol.* 179: 239–245.
51. Manser, E., T. Leung, H. Saliuddin, Z. S. Zhao, and L. Lim. 1994. A brain serine/threonine protein kinase activated by Cdc42 and Rac1. *Nature* 367: 40–46.
52. Knaus, U. G., S. Morris, H. J. Dong, J. Chernoff, and G. M. Bokoch. 1995. Regulation of human leukocyte p21-activated kinases through G protein-coupled receptors. *Science* 269: 221–223.
53. Ding, J., U. G. Knaus, J. P. Lian, G. M. Bokoch, and J. A. Badwey. 1996. The renaturable 69- and 63-kDa protein kinases that undergo rapid activation in chemoattractant-stimulated guinea pig neutrophils are p21-activated kinases. *J. Biol. Chem.* 271: 24869–24873.
54. Bokoch, G. M. 2003. Biology of the p21-activated kinases. *Annu. Rev. Biochem.* 72: 743–781.
55. Zhao, Z. S., E. Manser, X. Q. Chen, C. Chong, T. Leung, and L. Lim. 1998. A conserved negative regulatory region in α PAK: inhibition of PAK kinases reveals their morphological roles downstream of Cdc42 and Rac1. *Mol. Cell Biol.* 18: 2153–2163.
56. Zenke, F. T., C. C. King, B. P. Bohl, and G. M. Bokoch. 1999. Identification of a central phosphorylation site in p21-activated kinase regulating autoinhibition and kinase activity. *J. Biol. Chem.* 274: 32565–32573.
57. Lei, M., W. Lu, W. Meng, M. C. Parrini, M. J. Eck, B. J. Mayer, and S. C. Harrison. 2000. Structure of PAK1 in an autoinhibited conformation reveals a multistage activation switch. *Cell* 102: 387–397.
58. Parrini, M. C., M. Lei, S. C. Harrison, and B. J. Mayer. 2002. Pak1 kinase homodimers are autoinhibited in trans and dissociated upon activation by Cdc42 and Rac1. *Mol. Cell* 9: 73–83.
59. Hoffman, G. R., and R. A. Cerione. 2000. Flipping the switch: the structural basis for signaling through the CRIB motif. *Cell* 102: 403–406.
60. Morreale, A., M. Venkatesan, H. R. Mott, D. Owen, D. Nietlispach, P. N. Lowe, and E. D. Laue. 2000. Structure of Cdc42 bound to the GTPase binding domain of PAK. *Nat. Struct. Biol.* 7: 384–388.
61. Chong, C., L. Tan, L. Lim, and E. Manser. 2001. The mechanism of PAK activation: autophosphorylation events in both regulatory and kinase domains control activity. *J. Biol. Chem.* 276: 17347–17353.
62. Buchwald, G., E. Hostinova, M. G. Rudolph, A. Kraemer, A. Sickmann, H. E. Meyer, K. Scheffzek, and A. Wittinghofer. 2001. Conformational switch and role of phosphorylation in PAK activation. *Mol. Cell Biol.* 21: 5179–5189.
63. King, C. C., E. M. Gardiner, F. T. Zenke, B. P. Bohl, A. C. Newton, B. A. Hemmings, and G. M. Bokoch. 2000. p21-activated kinase (PAK1) is phosphorylated and activated by 3-phosphoinositide-dependent kinase-1 (PDK1). *J. Biol. Chem.* 275: 41201–41209.
64. Yu, J. S., W. J. Chen, M. H. Ni, W. H. Chan, and S. D. Yang. 1998. Identification of the regulatory autophosphorylation site of autophosphorylation-dependent protein kinase (auto-kinase): evidence that auto-kinase belongs to a member of the p21-activated kinase family. *Biochem. J.* 334: 121–131.
65. Bagrodia, S., B. Dérizjard, R. J. Davis, and R. A. Cerione. 1995. Cdc42 and PAK-mediated signaling leads to Jun kinase and p38 mitogen-activated protein kinase activation. *J. Biol. Chem.* 270: 27995–27998.
66. Zhang, S., J. Han, M. A. Sells, J. Chernoff, U. G. Knaus, R. J. Ulevitch, and G. M. Bokoch. 1995. Rho family GTPases regulate p38 mitogen-activated protein kinase through the downstream mediator Pak1. *J. Biol. Chem.* 270: 23934–23936.
67. Gallagher, E. D., S. Xu, C. Moomaw, C. A. Slaughter, and M. H. Cobb. 2002. Binding of JNK/SAPK to MEKK1 is regulated by phosphorylation. *J. Biol. Chem.* 277: 45785–45792.
68. Chaudhary, A., W. G. King, M. D. Mattaliano, J. A. Frost, B. Diaz, D. K. Morrison, M. H. Cobb, M. S. Marshall, and J. S. Brugge. 2000. Phosphatidylinositol 3-kinase regulates Raf1 through Pak phosphorylation of serine 338. *Curr. Biol.* 10: 551–554.
69. Zang, M., C. Hayne, and Z. Luo. 2002. Interaction between active Pak1 and Raf-1 is necessary for phosphorylation and activation of Raf-1. *J. Biol. Chem.* 277: 4395–4405.
70. Manser, E., H. Y. Huang, T. H. Loo, X. Q. Chen, J. M. Dong, T. Leung, and L. Lim. 1997. Expression of constitutively active α -PAK reveals effects of the kinase on actin and focal complexes. *Mol. Cell Biol.* 17: 1129–1143.
71. Frost, J. A., A. Khokhlatchev, S. Stjepic, M. A. White, and M. H. Cobb. 1998. Differential effects of PAK1-activating mutations reveal activity-dependent and -independent effects on cytoskeletal regulation. *J. Biol. Chem.* 273: 28191–28198.
72. Sells, M. A., A. Pfaff, and J. Chernoff. 2000. Temporal and spatial distribution of activated Pak1 in fibroblasts. *J. Cell Biol.* 151: 1449–1458.
73. Shalom-Barak, T., and U. G. Knaus. 2002. A p21-activated kinase-controlled metabolic switch up-regulates phagocyte NADPH oxidase. *J. Biol. Chem.* 277: 40659–40665.
74. Eblen, S. T., J. K. Slack, M. J. Weber, and A. D. Catling. 2002. Rac-PAK signaling stimulates extracellular signal-regulated kinase (ERK) activation by regulating formation of MEK1-ERK complexes. *Mol. Cell Biol.* 22: 6023–6033.
75. Frost, J. A., H. Steen, P. Shapiro, T. Lewis, N. Ahn, P. E. Shaw, and M. H. Cobb. 1997. Cross-cascade activation of ERKs and ternary complex factors by Rho family proteins. *EMBO J.* 16: 6426–6438.
76. Dewas, C., M. Fay, M. A. Gougerot-Pocidalo, and J. El-Benna. 2000. The mitogen-activated protein kinase extracellular signal-regulated kinase 1/2 pathway is involved in formyl-methionyl-leucyl-phenylalanine-induced p47^{phox} phosphorylation in human neutrophils. *J. Immunol.* 165: 5238–5244.
77. Nick, J. A., N. J. Avdi, S. K. Young, C. Knall, P. Gerwins, G. L. Johnson, and G. S. Worthen. 1997. Common and distinct intracellular signaling pathways in human neutrophils utilized by platelet activating factor and fMLP. *J. Clin. Invest.* 99: 975–986.
78. Zu, Y. L., J. Qi, A. Gilchrist, G. A. Fernandez, D. Vazquez-Abad, D. L. Kreutzer, C. K. Huang, and R. I. Sha'afi. 1998. p38 mitogen-activated protein kinase activation is required for human neutrophil function triggered by TNF- α or fMLP stimulation. *J. Immunol.* 160: 1982–1989.
79. Sakamoto, K., F. Kuribayashi, M. Nakamura, and K. Takeshige. 2006. Involvement of p38 MAP kinase in not only activation of the phagocyte NADPH oxidase induced by formyl-methionyl-leucyl-phenylalanine but also determination of the extent of the activity. *J. Biochem.* 140: 739–745.
80. El Benna, J., J. Han, J. W. Park, E. Schmid, R. J. Ulevitch, and B. M. Babior. 1996. Activation of p38 in stimulated human neutrophils: phosphorylation of the oxidase component p47^{phox} by p38 and ERK but not by JNK. *Arch. Biochem. Biophys.* 334: 395–400.
81. Crespo, P., K. E. Schuebel, A. A. Ostrom, J. S. Gutkind, and X. R. Bustelo. 1997. Phosphotyrosine-dependent activation of Rac-1 GDP/GTP exchange by the vav proto-oncogene product. *Nature* 385: 169–172.
82. Kim, C., C. C. Marchal, J. Penninger, and M. C. Dinuer. 2003. The hemopoietic Rho/Rac guanine nucleotide exchange factor Vav1 regulates *N*-formyl-methionyl-leucyl-phenylalanine-activated neutrophil functions. *J. Immunol.* 171: 4425–4430.
83. Welch, H. C., W. J. Coadwell, C. D. Ellison, G. J. Ferguson, S. R. Andrews, H. Erdjument-Bromage, P. Tempst, P. T. Hawkins, and L. R. Stephens. 2002. P-Rex1, a PtdIns(3,4,5)P₃- and G β γ -regulated guanine-nucleotide exchange factor for Rac. *Cell* 108: 809–821.
84. Welch, H. C., A. M. Condliffe, L. J. Milne, G. J. Ferguson, K. Hill, L. M. Webb, K. Okkenhaug, W. J. Coadwell, S. R. Andrews, M. Thelen, et al. 2005. P-Rex1 regulates neutrophil function. *Curr. Biol.* 15: 1867–1873.
85. Diekmann, D., A. Abo, C. Johnston, A. W. Segal, and A. Hall. 1994. Interaction of Rac with p67^{phox} and regulation of phagocytic NADPH oxidase activity. *Science* 265: 531–533.
86. Dorseuil, O., L. Reibel, G. M. Bokoch, J. Camonis, and G. Gacon. 1996. The Rac target NADPH oxidase p67^{phox} interacts preferentially with Rac2 rather than Rac1. *J. Biol. Chem.* 271: 83–88.
87. Ming, W., S. Li, D. D. Billadeau, L. A. Quilliam, and M. C. Dinuer. 2007. The Rac effector p67^{phox} regulates phagocyte NADPH oxidase by stimulating Vav1 guanine nucleotide exchange activity. *Mol. Cell Biol.* 27: 312–323.
88. Wang, F., P. Herzmark, O. D. Weiner, S. Srinivasan, G. Servant, and H. R. Bourne. 2002. Lipid products of PI(3)Ks maintain persistent cell polarity and directed motility in neutrophils. *Nat. Cell Biol.* 4: 513–518.
89. Zhao, T., P. Nalbant, M. Hoshino, X. Dong, D. Wu, and G. M. Bokoch. 2007. Signaling requirements for translocation of P-Rex1, a key Rac2 exchange factor involved in chemoattractant-stimulated human neutrophil function. *J. Leukoc. Biol.* 81: 1127–1136.
90. Gardiner, E. M., K. N. Pestonjamas, B. P. Bohl, C. Chamberlain, K. M. Hahn, and G. M. Bokoch. 2002. Spatial and temporal analysis of Rac activation during live neutrophil chemotaxis. *Curr. Biol.* 12: 2029–2034.
91. Servant, G., O. D. Weiner, P. Herzmark, T. Balla, J. W. Sedat, and H. R. Bourne. 2000. Polarization of chemoattractant receptor signaling during neutrophil chemotaxis. *Science* 287: 1037–1040.

92. Weiner, O. D., P. O. Neilsen, G. D. Prestwich, M. W. Kirschner, L. C. Cantley, and H. R. Bourne. 2002. A PtdInsP₃- and Rho GTPase-mediated positive feedback loop regulates neutrophil polarity. *Nat. Cell Biol.* 4: 509–513.
93. Lawson, C. D., S. Donald, K. E. Anderson, D. T. Patton, and H. C. Welch. 2011. P-Rex1 and Vav1 cooperate in the regulation of formyl-methionyl-leucyl-phenylalanine-dependent neutrophil responses. *J. Immunol.* 186: 1467–1476.
94. Etienne-Manneville, S. 2004. Cdc42: the centre of polarity. *J. Cell Sci.* 117: 1291–1300.
95. Franca-Koh, J., and P. N. Devreotes. 2004. Moving forward: mechanisms of chemoattractant gradient sensing. *Physiology (Bethesda)* 19: 300–308.
96. Cau, J., and A. Hall. 2005. Cdc42 controls the polarity of the actin and microtubule cytoskeletons through two distinct signal transduction pathways. *J. Cell Sci.* 118: 2579–2587.
97. Van Keymeulen, A., K. Wong, Z. A. Knight, C. Govaerts, K. M. Hahn, K. M. Shokat, and H. R. Bourne. 2006. To stabilize neutrophil polarity, PIP3 and Cdc42 augment RhoA activity at the back as well as signals at the front. *J. Cell Biol.* 174: 437–445.
98. Phillipson, M., B. Heit, P. Colarusso, L. Liu, C. M. Ballantyne, and P. Kubers. 2006. Intraluminal crawling of neutrophils to emigration sites: a molecularly distinct process from adhesion in the recruitment cascade. *J. Exp. Med.* 203: 2569–2575.
99. Smith, C. W., S. D. Marlin, R. Rothlein, C. Toman, and D. C. Anderson. 1989. Cooperative interactions of LFA-1 and Mac-1 with intercellular adhesion molecule-1 in facilitating adherence and transendothelial migration of human neutrophils in vitro. *J. Clin. Invest.* 83: 2008–2017.
100. Patcha, V., J. Wigren, M. E. Winberg, B. Rasmussen, J. Li, and E. Särndahl. 2004. Differential inside-out activation of beta2-integrins by leukotriene B4 and fMLP in human neutrophils. *Exp. Cell Res.* 300: 308–319.
101. Miranti, C. K., and J. S. Brugge. 2002. Sensing the environment: a historical perspective on integrin signal transduction. *Nat. Cell Biol.* 4: E83–E90.
102. Qu, A., and D. J. Leahy. 1995. Crystal structure of the I-domain from the CD11a/CD18 (LFA-1, $\alpha_L\beta_2$) integrin. *Proc. Natl. Acad. Sci. USA* 92: 10277–10281.
103. McDowall, A., B. Leitinger, P. Stanley, P. A. Bates, A. M. Randi, and N. Hogg. 1998. The I domain of integrin leukocyte function-associated antigen-1 is involved in a conformational change leading to high affinity binding to ligand intercellular adhesion molecule 1 (ICAM-1). *J. Biol. Chem.* 273: 27396–27403.
104. Shimaoka, M., C. Lu, R. T. Palframan, U. H. von Andrian, A. McCormack, J. Takagi, and T. A. Springer. 2001. Reversibly locking a protein fold in an active conformation with a disulfide bond: integrin α_L I domains with high affinity and antagonist activity in vivo. *Proc. Natl. Acad. Sci. USA* 98: 6009–6014.
105. Carman, C. V., and T. A. Springer. 2003. Integrin avidity regulation: are changes in affinity and conformation underemphasized? *Curr. Opin. Cell Biol.* 15: 547–556.
106. Stewart, M., and N. Hogg. 1996. Regulation of leukocyte integrin function: affinity vs. avidity. *J. Cell. Biochem.* 61: 554–561.
107. Grabovsky, V., S. Feigelson, C. Chen, D. A. Bleijs, A. Peled, G. Cinamon, F. Baleux, F. Arenzana-Seisdedos, T. Lapidot, R. R. Lobb, and R. Alon; van Kooyk Y. 2000. Subsecond induction of α_4 integrin clustering by immobilized chemokines stimulates leukocyte tethering and rolling on endothelial vascular cell adhesion molecule 1 under flow conditions. *J. Exp. Med.* 192: 495–506.
108. Abram, C. L., and C. A. Lowell. 2009. The ins and outs of leukocyte integrin signaling. *Annu. Rev. Immunol.* 27: 339–362.
109. Mócsai, A., M. Zhou, F. Meng, V. L. Tybulewicz, and C. A. Lowell. 2002. Syk is required for integrin signaling in neutrophils. *Immunity* 16: 547–558.
110. Gakidis, M. A., X. Cullere, T. Olson, J. L. Wilsbacher, B. Zhang, S. L. Moores, K. Ley, W. Swat, T. Mayadas, and J. S. Brugge. 2004. Vav GEFs are required for β_2 integrin-dependent functions of neutrophils. *J. Cell Biol.* 166: 273–282.